Evidence that the C-Terminus of the D1 Polypeptide of Photosystem II is Ligated to the Manganese Ion that Undergoes Oxidation During the S_1 to S_2 Transition: An Isotope-Edited FTIR Study†

Hsiu-An Chu,[‡,§,#] Warwick Hillier,[§,⊥] and Richard J. Debus*[,‡]

Department of Biochemistry, University of California, Riverside, California 92521-0129, and Department of Chemistry, Michigan State University, East Lansing, Michigan 48824

Received October 28, 2003; Revised Manuscript Received January 27, 2004

ABSTRACT: Isotope-edited FTIR difference spectroscopy was employed to determine if the C-terminal α-COO^- group of the D1 polypeptide ligates the $(Mn)_4$ cluster in photosystem II (PSII) and, if so, if it ligates the Mn ion that undergoes an oxidation during the $S_1 \rightarrow S_2$ transition. Wild-type and mutant cells of the cyanobacterium *Synechocystis* sp. PCC 6803 were propagated photoautotrophically in the presence of L-[1-^{13}C]alanine or unlabeled (^{12}C) L-alanine. In wild-type cells, both the C-terminal α-COO^- group of the D1 polypeptide at D1-Ala344 and all alanine-derived peptide carbonyl groups will be labeled. In D1-A344G and D1-A344S mutant cells, the C-terminal α-COO^- group of the D1 polypeptide will *not* be labeled because this group is no longer provided by alanine. The resultant S_2-*minus*-S_1 FTIR difference spectra of purified wild-type and mutant PSII particles showed that one symmetric carboxylate stretching mode that is altered during the $S_1 \rightarrow S_2$ transition is sensitive to L-[1-^{13}C]alanine-labeling in wild-type PSII particles but not in D1-A344G and D1-A344S PSII particles. Because the only carboxylate group that can be labeled in the wild-type PSII particles but not in the mutant PSII particles is the C-terminal α-COO^- group of the D1 polypeptide, we assign the L-[1-^{13}C]alanine-sensitive symmetric carboxylate stretching mode to the α-COO^- group of D1-Ala344. In unlabeled wild-type PSII particles, this mode appears at ∼1356 cm^{-1} in the S_1 state and at ∼1339 or ∼1320 cm^{-1} in the S_2 state. These frequencies are consistent with unidentate ligation of the $(Mn)_4$ cluster by the α-COO^- group of D1-Ala344 in both the S_1 and S_2 states. The apparent 17−36 cm^{-1} downshift in frequency in response to the $S_1 \rightarrow S_2$ transition is consistent with the α-COO^- group of D1-Ala344 ligating a Mn ion whose charge increases during the $S_1 \rightarrow S_2$ transition. Accordingly, we propose that the α-COO^- group of D1-Ala344 ligates the Mn ion that undergoes an oxidation during the $S_1 \rightarrow S_2$ transition. Control experiments were conducted with Mn-depleted wild-type PSII particles. These experiments showed that tyrosine Y_D may be structurally coupled to the carbonyl oxygen of an alanine-derived peptide carbonyl group.

The catalytic site of water oxidation in photosystem II (PSII)[1] contains a cluster of four Mn ions that interacts closely with a redox-active tyrosine residue known as Y_Z (for reviews, see refs *1*−*9*). One Ca ion and one Cl ion are required for catalytic activity and appear to be located close to the $(Mn)_4$ cluster (*10*, *11*). The $(Mn)_4$ cluster accumulates oxidizing equivalents in response to light-induced electron-transfer reactions within PSII, thereby providing the interface between one-electron photochemistry and the four-electron process of water oxidation. Tyrosine Y_Z serves as the immediate oxidant of the $(Mn)_4$ cluster, transferring an electron from the $(Mn)_4$ cluster to $P_{680}^{\bullet+}$ in response to the light-induced formation of the latter. Photosystem II also contains a second redox-active tyrosine residue, known as Y_D. Tyrosine Y_D can rapidly reduce $P_{680}^{\bullet+}$ (*12*), but it is not involved in the normal catalytic reactions of water oxidation. The function of Y_D is unclear, although the presence of $Y_D^{\bullet}$

† This work was supported by the National Science Foundation (MCB 0111065 to R.J.D.) and the National Institutes of Health (GM37300 to Gerald T. Babcock[§]) and is dedicated to the memory of Gerald T. Babcock.

* To whom correspondence should be addressed. Phone: (909) 787-3483, Fax: (909) 787-4434, E-mail: richard.debus@ucr.edu.

‡ University of California.

§ Michigan State University.

⊥ Present Address: Research School of Biological Sciences, Australian National University, GPO Box 475, Canberra ACT, Australia 2601.

Present Address: Institute of Botany, Academia Sinica, Taipei, Taiwan, 11529, Republic of China.

[1] Abbreviations: BChl, bacteriochlorophyll; Car, *β*-carotene; Chl, chlorophyll; Cyt, cytochrome; DCMU, 3-(3,4-dichlorophenyl)-1,1-dimethylurea; EDTA, ethylenediaminetetraacetic acid; ENDOR, electron nuclear double resonance; EPR, electron paramagnetic resonance; ESEEM, electron spin−echo envelope modulation; EXAFS, extended X-ray absorption fine structure; FTIR, Fourier transform infrared; GC/MS, gas chromatography/mass spectrometry; MES, 2-(*N*-morpholino)-ethanesulfonic acid; NTA, nitrilotriacetic acid; P_{680}, chlorophyll species that serves as the light-induced electron donor in PSII; PSII, photosystem II; Q_A, primary plastoquinone electron acceptor; TES, *N*-tris-(hydroxymethyl)methyl-2-aminoethanesulfonic acid; wild-type*, control strain of *Synechocystis* sp. PCC 6803 that was constructed in the same manner as the D1-A344G and D1-A344S mutants but that contains the wild-type *psb*A-2 gene; Y_Z, tyrosine residue that mediates electron transfer between the $(Mn)_4$ cluster and $P_{680}^{\bullet+}$; Y_D, second tyrosine residue that can reduce $P_{680}^{\bullet+}$ in PSII; XANES, X-ray absorption near edge structure.

10.1021/bi035915f CCC: $27.50
Published on Web 02/27/2004

appears to increase the reduction potential of $P_{680}^{\bullet+}/P_{680}$ (*8*, *12*, *13*), influence the localization of the $P_{680}^{\bullet+}$ cation between the Chl molecules that comprise P_{680} (*8*, *12*), and accelerate the assembly of the $(Mn)_4$ cluster (*13*).

During each catalytic cycle, the $(Mn)_4$ cluster cycles through five oxidation states termed S_n, where "*n*" denotes the number of oxidizing equivalents that have been stored. The S_1 state predominates in dark-adapted samples. Most interpretations of XANES data have concluded that the S_1 state consists of two Mn(III) and two Mn(IV) ions and that the S_2 state consists of one Mn(III) and three Mn(IV) ions (*2*, *3*, *14*−*16*), but an alternative view exists (*17*, *18*). The additional oxidizing equivalent of the S_3 state may be localized on a Mn ligand (refs *16* and *19*, but see ref *15*). The S_4 state is a transient intermediate (possibly corresponding to the $Y_Z^{\bullet}S_3$ state) that reverts to the S_0 state with the concomitant release of O_2.

The electron density of the Mn cluster is visible in the recent 3.6−3.8 Å crystal structures of PSII (*20*−*22*). However, the exact arrangement of the four Mn ions is unknown. The resolutions of the current X-ray data are not sufficient to provide this information. Nevertheless, EXAFS studies have detected the presence of two to three Mn−Mn interactions with distances of ∼2.7 Å and at least one Mn−Mn and/or Mn−Ca interaction with a distance of ∼3.3 Å (*2*, *3*, *14*−*16*). These distances, along with recent simulations of EPR and ENDOR data of samples poised in the S_2 state, have provided families of possible arrangements for the $(Mn)_4$ cluster, predicting it to be a tetramer consisting of three strongly exchange-coupled Mn ions that are weakly exchange-coupled to a fourth Mn ion (*23*, *24*). These arrangements are compatible with the recent 3.6−3.8 Å crystal structures.

On the basis of numerous site-directed mutagenesis and biochemical studies, most or all of the amino acid residues that ligate the $(Mn)_4$ cluster are expected to be contributed by the D1 polypeptide (for reviews, see refs *25*−*27*). The recent 3.6−3.8 Å crystal structures are consistent with this expectation (*20*−*22*), but the resolutions of these structures are insufficient to unambiguously identify the individual protein ligands. The residues that have been identified as potential Mn ligands by the mutagenesis and biochemical studies are D1-Asp170, D1-His190, D1-His332, D1-Glu333, D1-His337, D1-Asp342, and the C-terminus of the D1 polypeptide at Ala344. Most or all of these residues are consistent with the most recent crystallographic structural analyses (*21*, *22*). The original mutagenesis studies were conducted with intact cells of *Synechocystis* sp. PCC 6803 or *Chlamydomonas reinhardtii*. More recently, 9.2 GHz ESEEM studies of PSII particles purified from the *Synechocystis* mutants D1-H332E and D1-D170H provided strong evidence for the ligation of the $(Mn)_4$ cluster by D1-His332 (*28*), but provided no definitive evidence for or against the ligation of the $(Mn)_4$ cluster by D1-Asp170 (*29*). Nevertheless, a recent FTIR study of *Synechocystis* D1-D170H PSII particles showed that a low-frequency Mn−O−Mn vibrational mode that appears at ∼606 cm^{-1} in the S_2 state shifts to ∼612 cm^{-1} in the mutant, showing that D1-Asp170 is structurally coupled to the $(Mn)_4$ cluster (*30*).

FTIR difference spectroscopy is an extremely sensitive technique for characterizing dynamic structural changes that occur during an enzyme's catalytic cycle, such as changes in molecular interactions, protonation states, bonding (including changes in metal coordination and hydrogen bonding), bond strengths, and protein backbone conformations (*31*−*34*). In PSII, numerous vibrational modes change as the $(Mn)_4$ cluster is oxidized through the S state cycle (for reviews, see refs *35* and *36*). Many of these vibrational modes correspond to amino acid residues that either ligate the $(Mn)_4$ cluster, are coupled to the $(Mn)_4$ cluster through hydrogen bonds, interact electrostatically with the $(Mn)_4$ cluster, or have side chains whose protonation states change as the $(Mn)_4$ cluster is oxidized. The mid-frequency region (2000−1000 cm^{-1}) of the S_2-*minus*-S_1 FTIR difference spectrum of PSII contains numerous bands that have been attributed to carboxylate stretching modes. Negative bands at ∼1560 and ∼1402 cm^{-1} and positive bands at ∼1588 and ∼1364 cm^{-1} have been assigned to a Mn-ligating carboxylate group whose coordination mode changes from bridging or bidentate chelating to unidentate during the $S_1 \rightarrow S_2$ transition (*37*, *38*). A negative band at ∼1561 cm^{-1} has been assigned to the asymmetric stretching mode of a carboxylate group that forms a hydrogen bond with a Mn-bound water molecule (*39*). These carboxylate bands shift 20−45 cm^{-1} to lower frequencies in samples that have been uniformly labeled with ^{13}C (*40*−*42*). Additional negative bands at ∼1254 and ∼1521 cm^{-1} have been assigned to a tyrosine residue (presumed to be Y_Z) that is structurally coupled to the $(Mn)_4$ cluster (*43*). Another negative band at ∼1113 cm^{-1} has been assigned to a histidine residue that either ligates the $(Mn)_4$ cluster or is structurally coupled to it through a network of hydrogen bonds (*44*). However, none of the vibrational features that have been observed in the mid-frequency S_2-*minus*-S_1 FTIR difference spectrum of PSII has yet been correlated with an individual amino acid residue in PSII with the exception of the bands that have been assigned tentatively to Y_Z (*43*).

Identifying the vibrational modes that change during the S state cycle in PSII will provide information about S state-dependent protein structural changes. This information is crucial to understanding the mechanism of water oxidation and will complement the information that will be obtained from X-ray crystallography. In this study, we have employed FTIR difference spectroscopy in an attempt to determine if the free carboxylate (α-COO^-) of Ala344 at the C-terminus of the D1 polypeptide ligates the assembled $(Mn)_4$ cluster and, if so, to determine if it ligates the Mn ion that undergoes an oxidization during the $S_1 \rightarrow S_2$ transition. The proposal that the free carboxylate of D1-Ala344 ligates the $(Mn)_4$ cluster was advanced by Diner and co-workers in 1992 on the basis of a study of intact mutant cells of *Synechocystis* sp. PCC 6803 having truncated or unprocessed C-termini [e.g., the mutants A344stop and S345P (*45*)]. The most recent crystallographic structural analyses show that the C-terminal region of the D1 polypeptide is located in close proximity to the $(Mn)_4$ cluster and are consistent with this proposal (*21*, *22*). To test this proposal, the mid-frequency S_2-*minus*-S_1 FTIR difference spectrum of L-[1-^{13}C]alanine-labeled *Synechocystis* PSII particles was obtained to see if the vibrational modes that are altered during the $S_1 \rightarrow S_2$ transition include those of the α-COO^- moiety of D1-Ala344. In *Synechocystis* sp. PCC 6803, the only known or suspected PSII subunits (*46*) that have C-terminal Ala residues are D1, CP47, and psbY (*47*, *48*) (see the CyanoBase genome database at http://www.kazusa.or.jp/cyano/cyano.html). The

C-termini of the CP47 and psbY polypeptides are located on the stromal side of the thylakoid membrane. Furthermore, the C-terminus of the CP47 polypeptide is provided by a hexa-histidine tag in the *Synechocystis* strains that are described in this study (*28*). Consequently, neither polypeptide has a C-terminal alanine residue that can interact with the $(Mn)_4$ cluster. Nevertheless, to differentiate the α-COO^- group of D1-Ala344 from the α-COO^- group of any other PSII subunit that might have a C-terminal alanine residue, and to differentiate the carboxylate modes of the α-COO^- group of D1-Ala344 from the amide modes of alanine-derived peptide carbonyl groups, the S_2-*minus*-S_1 FTIR difference spectrum of wild-type* PSII particles was compared with those of PSII particles isolated from the *Synechocystis* mutants D1-A344G and D1-A344S. Cells were propagated photoautotrophically in the presence of either L-[1-^{13}C]alanine or unlabeled (^{12}C) L-alanine. In wild-type* PSII particles, the C-terminal α-COO^- group of the D1 and psbY polypeptides will be labeled, as will all alanine-derived peptide carbonyl groups. In D1-A344G and D1-A344S PSII particles, the C-terminal α-COO^- group of the D1 polypeptide will *not* be labeled because it is not provided by alanine. Our results show that the C-terminal carboxylate of the D1 polypeptide is structurally coupled to the $(Mn)_4$ cluster. Further, our results are consistent with the α-COO^- carboxylate of D1-Ala344 serving as a unidentate ligand of the $(Mn)_4$ cluster in both the S_1 and S_2 states, and, more specifically, serving as a unidentate ligand of a Mn ion whose charge increases during the $S_1 \rightarrow S_2$ transition. We propose that this is the Mn ion that undergoes an oxidation during the $S_1 \rightarrow S_2$ transition. A preliminary account of this study has been presented (*49*).

MATERIALS AND METHODS

Construction of Site-Directed Mutants. The D1-A344G and D1-A344S mutations were constructed in the *psbA-2* gene of the glucose-tolerant variant (*48*, *50*) of *Synechocystis* sp. PCC 6803 following methods that were described previously (*51*). To avoid potential problems with the posttranslational processing of the D1 polypeptide's C-terminal extension (*45*), each mutation was accompanied by others that changed the D1-Ser345 codon to a stop codon (*52*). Mutation-bearing plasmids were transformed into a host strain of *Synechocystis* that lacks all three *psbA* genes (*53*) and contains a hexa-histidine tag on the carboxy terminus of CP47 (*28*). Single colonies were selected for their ability to grow on solid media containing 5 μg/mL kanamycin monosulfate (*53*) and 20 μg/mL gentamycin sulfate (*28*). The control wild-type* strain was constructed in the same manner except that the transforming plasmid carried no site-directed mutations. The designation "wild-type*" differentiates this strain from the native glucose-tolerant wild-type strain (*48*, *50*) that contains all three *psb*A genes and is sensitive to antibiotics.

Propagation of Cultures. The wild-type* and mutant cells were maintained on solid growth media at 30 °C under constant illumination [fluorescent cool-while bulbs at an intensity of 50−60 μE m^{-2} s^{-1} (*54*)]. The solid media consisted of BG-11 (*55*) containing 1.5% (w/v) Difco Bacto-Agar (Becton Dickinson & Co., Sparks, MD), 10 mM TES−NaOH (pH 8.0), 0.3% (w/v) sodium thiosulfate, 5 mM glucose, 10 μM DCMU, 5 μg/mL kanamycin monosulfate, and 20 μg/mL gentamycin sulfate. The liquid media consisted of BG-11 (*55*) containing 5 mM TES−NaOH (pH 8.0) and was supplemented as indicated below. During cell growth, the liquid growth media was aerated by bubbling with sterile, humidified air. For the isolation of isotopically labeled PSII particles, cells were first propagated photoautotrophically in liquid media held in two modified 250-mL Erlenmeyer flasks (*54*) at the same temperature and under the same illumination conditions as the solid media until they reached an optical density of 0.9−1.2 at 730 nm. About 20 mL of these cultures were used to inoculate each of 15−17 similarly modified Erlenmeyer flasks each holding ∼1 L of growth medium containing either 0.5 mM unlabeled (^{12}C) L-alanine or 0.5 mM L-[1-^{13}C]alanine (99% ^{13}C enrichment, Cambridge Isotope Laboratories, Andover, MA) (*56*). These larger cultures were then propagated photoautotrophically under the same conditions as the smaller cultures until their optical densities reached 0.9−1.1 at 730 nm (typically 6−7 days). Optical densities were measured with a modified CARY 14 spectrophotometer (OLIS, Inc., Bogart, GA).

Purification of PSII Particles. Isolated PSII particles were purified under dim green light at 4 °C with Ni−NTA superflow affinity resin (Qiagen, Valentia, CA) as described previously (*29*). The column flow-through was saved for analysis by mass spectrometry and the purified PSII particles were eluted with purification buffer [25% (v/v) glycerol, 50 mM MES−NaOH (pH 6.0), 20 mM $CaCl_2$, 5 mM $MgCl_2$, 0.03% (w/v) *n*-dodecyl β-D-maltoside] containing 50 mM L-histidine. After the addition of EDTA to 1 mM, the eluted PSII particles were concentrated to 0.5−1.0 mg of Chl/mL by ultrafiltration (*29*), frozen in liquid nitrogen, and stored at −80 °C. To prepare Mn-depleted PSII particles, O_2-evolving PSII particles were incubated at ∼0.25 mg of Chl/mL in the presence of 5 mM NH_2OH and 5 mM EDTA at 4 °C in darkness for 30 min (*57*). The extracted material was then adsorbed to a Pharmacia HR 5/5 Mono-Q ion-exchange column and washed extensively with purification buffer (15−20 column volumes) to remove the NH_2OH and extracted Mn ions. The column was then inverted (*58*) and eluted slowly with purification buffer containing 0.5 M NaCl. For the FTIR experiments, all PSII particles were transferred into sucrose buffer [0.4 M sucrose, 50 mM MES−NaOH (pH 6.0), 20 mM $CaCl_2$, 5 mM $MgCl_2$, 0.03% (w/v) *n*-dodecyl β-D-maltoside] by two cycles of concentration/dilution in Centricon-100 concentrators (Millipore Corp., Bedford, MA). During each cycle, the samples were concentrated to 5−7 mg of Chl/mL and then diluted ≥ 10-fold with sucrose buffer. This procedure served to decrease the concentrations of glycerol, L-histidine, and EDTA (or glycerol and NaCl, in the case of Mn-depleted PSII particles) by ≥100-fold. Finally, the samples were concentrated to 5−7 mg of Chl/mL, frozen in liquid nitrogen, and stored at −80 °C.

Mass Spectrometry. The flow-throughs from the Ni−NTA affinity column were adsorbed to a Pharmacia Q-Sepharose Fast Flow ion-exchange column, washed with purification buffer to remove excess *n*-dodecyl β-D-maltoside and other contaminants, eluted with purification buffer containing 0.5 M NaCl, passed through a Pharmacia HR 26/10 desalting column to remove the NaCl, then concentrated to 5−7 mg of Chl/mL by ultrafiltration followed by centrifugation in Centricon-100 concentrators (Millipore Corp., Bedford, MA). Aliquots were acetone precipitated, dried under vacuum, and

hydrolyzed with 6 N HCl vapor at 110 °C for 24 h in an atmosphere of nitrogen gas. After hydrolysis, the amino acids were dried under vacuum before being converted to their corresponding N,O(S)-*tert*-butyldimethylsilyl derivatives as described in ref *59*. The derivatized amino acid residues were subjected to GC/MS analysis with an HP 5890 II gas chromatograph and an HP 5972 mass spectrometer (Hewlett-Packard, Palo Alto, CA) as described previously (*60*). Single ion monitoring was used for the measurement of mass isotopomers.

Experimental Conditions for FTIR Measurements. All manipulations were conducted under dim green light at 4 °C. Thawed samples were diluted with two volumes of water and reconcentrated to 5−7 mg of Chl/mL with Microcon-100 concentrators (Millipore Corp., Bedford, MA). An aliquot (2−5 mL) of PSII was mixed into an equal volume of fresh 10 mM potassium ferricyanide (dissolved in water) on a 15- or 25-mm diameter CaF_2 or AgBr window. The sample was then dried lightly (until tacky) under a stream of dry nitrogen gas. To ensure that each sample contained the same moisture content, the partially dehydrated samples were immediately allowed to rehydrate in a controlled humidity chamber (90−92% relative humidity) for 12−15 min (*61*). A second IR window was then placed over the first and sealed with high-vacuum grease to prevent further sample dehydration in the FTIR cryostat. The sample was then loaded into the cryostat and allowed to equilibrate to 250.0 K, a process that typically required 1−4 h. The sample concentration and thickness were adjusted so that the absolute absorbance of the amide I band at 1657 cm^{-1} was 0.7−1.0.

FTIR Spectra. Mid-frequency FTIR spectra were recorded with a Bruker Equinox 55 spectrometer (Bruker Optics, Billerica, MA) that was equipped with a water-cooled globar source, a KBr beam splitter, a preamplified, midrange MCT detector (model D316/6, InfraRed Associates, Stuart, FL), and either a home-built liquid nitrogen cryostat (*30*, *62*) that was controlled with a Lake Shore 340 temperature controller (Lake Shore, Westerville, OH) or a commercial liquid nitrogen cryostat (Optistat DN, Oxford Instruments, Oxon, UK) that was controlled with an Oxford ITC502 temperature controller. These cryostats regulated the sample temperature to within ± 0.01 and ± 0.1 K, respectively. A 4000 cm^{-1} long-pass Ge filter (model FXLP-0400, Janos Technology, Townshend, VT) was mounted before the sample holder to reduce the spectral bandwidth and to prevent the interferometer's coaxial helium−neon laser beam from illuminating the sample. Double-sided forward−backward interferograms were recorded with a scanner velocity of 80 kHz (this corresponds to a mirror velocity of 2.5 cm/s). For the calculation of Fourier transforms, a Blackmann-Harris 3-term apodization function and a zero-fill factor of 4 were employed. The spectral resolution for all spectra was 4 cm^{-1}. Samples were illuminated with a single flash (7−9 mJ/flash, ∼7 ns fwhm) from a frequency-doubled Q-switched Nd:YAG laser [Quanta-Ray DCR-1 (Spectra-Physics, Mountain View, CA) or Surelite I (Continuum, Santa Clara, CA)]. Flash excitation was controlled from the Equinox 55 OPUS interface. The Nd:YAG laser was programmed to deliver a single Q-switched flash during a 10 or 20 Hz flashlamp repetition series to ensure the uniformity of the laser light intensity. For each sample, a preflash single-beam spectrum of 800 scans was acquired (the acquisition took ∼100 s), a single Q-switched laser flash was applied, a period of 10 s was allowed to elapse to facilitate the oxidation of $Q_A^{\bullet-}$ by ferricyanide (*44*, *63*, *64*), and then a post-flash single-beam spectrum of 800 scans was acquired (this acquisition also took ∼100 s). The post-flash spectrum was divided by the preflash spectrum and converted to units of absorbance to yield a true "light-*minus*-dark" absorbance difference spectrum. Each difference spectrum was acquired with a fresh sample. For O_2-evolving PSII particles (Figures 1 and 2), three to six difference spectra were averaged. For Mn-depleted PSII particles (Figure 4), 10−12 difference spectra were averaged. Absorption spectra of alanine were recorded at room temperature. Solutions of 2.5 mM alanine dissolved in 3 M NaOH were held between two AgBr windows. To remove the overlapping water band at 1657 cm^{-1}, the spectra were corrected by subtracting the spectrum of 3 M NaOH.

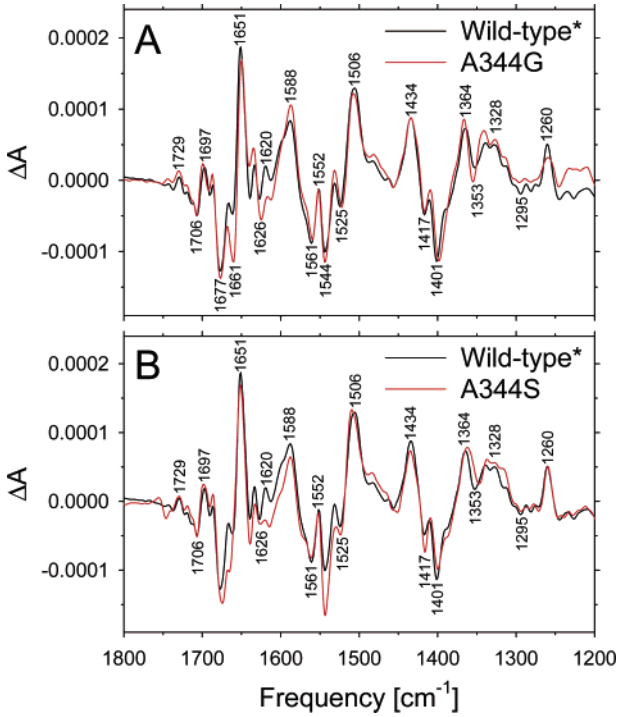

FIGURE 1: Comparison of the mid-frequency (1800−1200 cm^{-1}) flash-induced S_2-*minus*-S_1 FTIR difference spectra of wild-type*, D1-A344G, and D1-A344S PSII particles purified from *Synechocystis* cells propagated in the presence of unlabeled (^{12}C) L-alanine. A total of four, three, and five difference spectra were averaged for the wild-type*, D1-A344G, and D1-A344S traces, respectively. Panel A shows a comparison of the spectra of D1-A344G (red line) and wild-type* (black line) PSII particles. Panel B shows a comparison of the spectra of D1-A344S (red line) and wild-type* (black line) PSII particles. The same wild-type* spectrum is shown in each panel. Spectra have been normalized to maximize their overlap. All spectra were collected with a sample temperature of 250 K and a resolution of 4 cm^{-1}.

Other Procedures. Chlorophyll concentrations and light-saturated rates of O_2 evolution were measured as described previously (*54*, *57*).

RESULTS

The D1-A344G and D1-A344S mutants are photoautotrophic, as reported previously for *Synechocystis* sp. PCC 6803 (*45*) and as reported previously for the D1-A344S mutant of *Chlamydomonas reinhardtii* (*65*). The light-saturated rates of O_2 evolution exhibited by the purified wild-

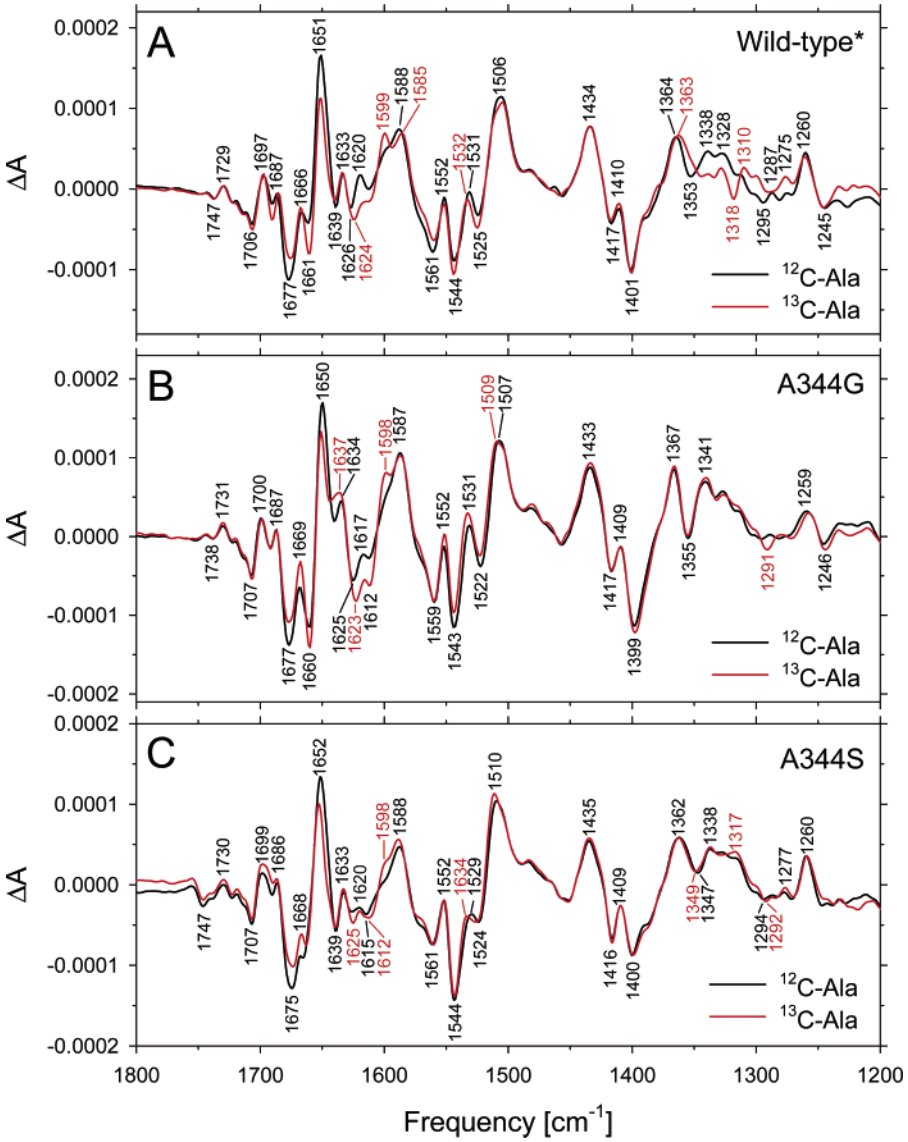

FIGURE 2: Comparison of the mid-frequency (1800−1200 cm^{-1}) flash-induced S_2-*minus*-S_1 FTIR difference spectra of (A) wild-type*, (B) D1-A344G, and (C) D1-A344S PSII particles purified from *Synechocystis* cells propagated in the presence of unlabeled (^{12}C) L-alanine (black lines) or L-[1-^{13}C]alanine (red lines). The spectra of the unlabeled wild-type*, D1-A344G, and D1-A344S PSII particles (black lines) are the same as those shown in Figure 2 and represent the averages of four, three, and five difference spectra, respectively. The spectra of the L-[1-^{13}C]alanine-labeled wild-type*, D1-A344G, and D1-A344S PSII particles (red lines) represent the averages of three, three, and six difference spectra, respectively. In each panel, the spectra have been normalized to maximize their overlap between 1500 and 1400 cm^{-1}. All spectra were collected with a sample temperature of 250 K and a resolution of 4 cm^{-1}.

type*, D1-A344G, and D1-A344S PSII particles were 3.5−4.1, 1.9−2.1, and 2.8−3.0 mM O_2 (mg of Chl)$^{-1}$ h^{-1}, respectively. Analysis by mass spectrometry of the Ni−NTA affinity column flow-throughs revealed that, for the L-[1-^{13}C]alanine-labeled preparations, the total incorporation of ^{13}C was 70 ± 2% for Ala (> 99% of this was at the C_1 position), 14 ± 4% for Val (~70% of this was at the C_1 position), 13 ± 4% for Phe (< 19% of this was at the C_1 position), 9 ± 4% for Tyr (< 26% of this was at the C_1 position), 6 ± 3% for Leu, and < 6% for all other amino acids examined (all were examined except Lys, Arg, Trp, and Cys). These data show that exogenous alanine is incorporated effectively into protein in *Synechocystis* with little equilibration into cellular pools of pyruvate and, therefore, with little incorporation into the carbonyl moieties of peptide groups other than those derived from alanine. The level of incorporation of ^{13}C into alanine is similar to the level of incorporation that was observed previously for *Synechocystis* cells that had been propagated in the presence of 0.5 mM [^{13}C]alanine (*56*).

The mid-frequency S_2-*minus*-S_1 FTIR difference spectra of unlabeled D1-A344G and D1-A344S PSII particles are compared to the spectrum of unlabeled wild-type* PSII particles in Figure 1, panels A and B, respectively. The differences between the mutant spectra (red lines) and the wild-type* spectrum (black lines) are subtle, showing that neither mutation significantly perturbs the structure of PSII.

Comparisons of the mid-frequency FTIR difference spectra of unlabeled and L-[1-^{13}C]alanine-labeled wild-type*, D1-A344G, and D1-A344S PSII particles are shown in Figure 2 (the spectra of labeled and unlabeled PSII particles are depicted with red and black lines, respectively). In the wild-type* PSII particles (Figure 2A), the incorporation of L-[1-^{13}C]alanine caused significant shifts of bands in the overlapping amide I stretching (1690−1620 cm^{-1}) and asymmetric carboxylate stretching (1640−1500 cm^{-1}) regions and in the

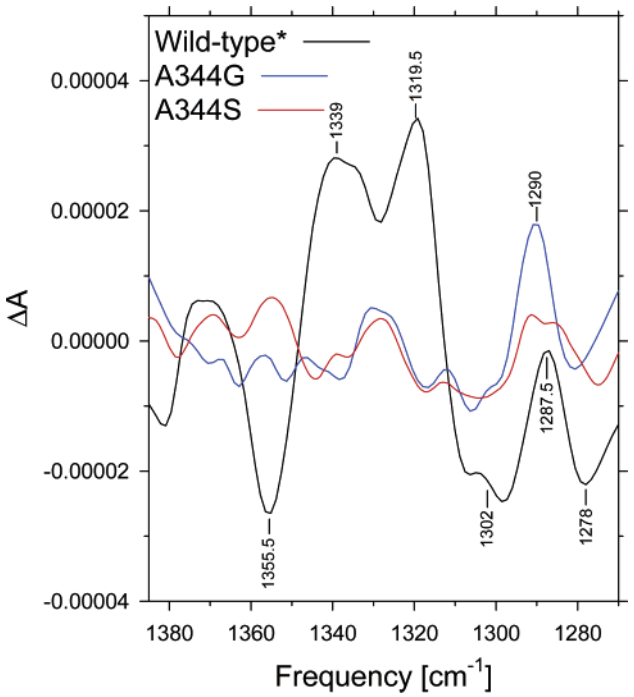

FIGURE 3: Double difference spectra, ^{12}C-*minus*-^{13}C, of wild-type* (black line), D1-A344G (blue line), and D1-A344S (red line) PSII particles obtained by subtracting the S_2-*minus*-S_1 FTIR difference spectra of [1-^{13}C]alanine-labeled PSII particles from the S_2-*minus*-S_1 FTIR difference spectra of unlabeled PSII particles (the spectra shown in Figure 2 were subtracted directly without adjustment). Only the regions between 1385 and 1270 cm^{-1} are shown.

symmetric carboxylate stretching region (1450−1300 cm^{-1}). However, in the D1-A344G and D1-A344S PSII particles (Figure 2, panels B and C, respectively), the incorporation of L-[1-^{13}C]alanine caused significant shifts only in the overlapping amide I/asymmetric carboxylate stretching regions. The L-[1-^{13}C]alanine-induced shifts that were observed between 1360 and 1260 cm^{-1} in the wild-type* spectrum (Figure 2A) were almost completely absent from the D1-A344G and D1-A344S spectra (Figure 2, panels B and C, respectively). To display the shifted modes more clearly, the ^{12}C-*minus*-^{13}C double difference spectrum of the region between 1385 and 1270 cm^{-1} is presented in Figure 3. For the wild-type* PSII particles (black line), the double-difference spectrum is consistent with a single S_1 state mode at ∼1355.5 cm^{-1} shifting to ∼1339 or ∼1319.5 cm^{-1} after the incorporation of L-[1-^{13}C]alanine, and with a single S_2 state mode at ∼1339 or ∼1319.5 cm^{-1} shifting to ∼1302 cm^{-1}. Note that these shifted modes do not appear in the double-difference spectra of the D1-A344G (blue line) or D1-A344S (red line) PSII particles.

A number of L-[1-^{13}C]alanine-induced shifts appear in the amide I stretching regions of both wild-type* and mutant PSII particles. Major features include an apparent shift of a positive feature from ∼1651 cm^{-1} and the appearance of a positive feature at ∼1599 cm^{-1}. To determine if one or more of the shifted bands arise from residual populations of PSII reaction centers that have lost the $(Mn)_4$ cluster during purification of the PSII particles, Mn-depleted wild-type* PSII particles were prepared containing unlabeled (^{12}C) L-alanine or L-[1-^{13}C]alanine. The flash-induced light-*minus*-dark FTIR difference spectra of these PSII particles are compared in Figure 4. The spectral features of the unlabeled Mn-depleted wild-type* PSII particles (black line) are completely different from those of intact PSII particles recorded under the same experimental conditions (Figures 1 and 2A, black lines), as shown previously (*64*, *66*). The spectrum was the same whether the $(Mn)_4$ cluster was extracted in the presence of EDTA or not (not shown). The spectrum of the L-[1-^{13}C]alanine-labeled Mn-depleted wild-type* PSII particles (red line in Figure 4) closely resembled that of the unlabeled wild-type* PSII particles except in the overlapping amide I/asymmetric carboxylate stretching regions. As in the intact PSII preparations, major features include the apparent shift of a positive feature from ∼1652 cm^{-1} and the appearance of a positive feature at ∼1601 cm^{-1}.

The spectra of unlabeled (^{12}C) L-alanine and L-[1-^{13}C]-alanine dissolved in 3 M NaOH are shown in Figure 5. In unlabeled (^{12}C) L-alanine, major bands appeared at 1559, 1459, 1414, and 1368 cm^{-1}, smaller features appeared between 1368 and 1292 cm^{-1}, and other bands appeared at 1238, 1138, and 1080 cm^{-1} (Figure 5, black trace). On the basis of previous experimental and normal-mode analyses of L-alanine and its deuterated analogues (*67*−*70*), the bands at 1559, 1459, and 1414 cm^{-1} can be assigned to the asymmetric carboxylate stretching mode [$\nu_{asym}(COO^-)$], the asymmetric methyl deformation mode [$\delta_{asym}(CH_3)$], and the symmetric carboxylate stretching mode [$\nu_{sym}(COO^-)$], respectively. The features between ∼1368 and ∼1292 cm^{-1} can be assigned to symmetric methyl deformation [$\delta_{sym}(CH_3)$] and methyne deformation [δ(CH)] modes (*67*−*70*). The $\delta_{sym}(CH_3)$ and δ(CH) modes are strongly coupled to the $\nu_{sym}(COO^-)$ mode. In L-[1-^{13}C]alanine, the $\nu_{asym}(COO^-)$ mode downshifts by ∼39 to 1520 cm^{-1} and the $\nu_{sym}(COO^-)$ mode downshifts by ∼18 to 1396 cm^{-1} (Figure 5, red trace). The features between 1368 and 1292 cm^{-1} are also downshifted in L-[1-^{13}C]alanine. The latter shifts are expected because both $\delta_s(CH_3)$ and δ(CH) are strongly coupled to $\nu_{sym}(COO^-)$.

DISCUSSION

The mid-frequency S_2-*minus*-S_1 FTIR difference spectrum of unlabeled wild-type* PSII particles that is presented in this work (Figures 1 and 2A, black lines) closely resembles the spectra that have been reported previously by several groups for *Synechocystis* sp. PCC 6803 (*30*, *42*−*44*), *Thermosynechococcus elongatus* (*40*, *41*, *64*, *71*−*73*), and spinach (*30*, *37*−*39*, *43*, *44*, *62*, *63*, *66*, *74*−*80*). The same spectral features have now been obtained with PSII preparations from three organisms and under a variety of experimental conditions [e.g., after short (*43*, *62*, *71*, *76*) or long (*37*, *39*, *74*, *75*) dark-adaptation times, at temperatures ranging from 200 K (*63*, *66*) to 250 K (*30*, *37*−*40*, *42*−*44*, *63*, *64*, *66*, *74*, *75*, *77*−*80*) to 265 K (*62*), to 283 K (*41*, *71*−*73*), to 289 K (*76*), in the presence of various concentrations of sucrose (*30*, *37*−*39*, *42*−*44*, *62*−*64*, *66*, *71*, *74*−*80*), in mixtures of cryoprotectants (*63*), or in the absence of cryoprotectants (*41*, *72*, *73*), and in both hydrated (*37*−*39*, *42*, *44*, *62*, *63*, *74*−*76*, *78*−*80*) and partially dehydrated (*30*, *41*, *43*, *44*, *64*, *66*, *71*−*73*, *77*) samples]. The features of this spectrum (and those of the other $S_n \rightarrow S_{n+1}$ transitions) oscillate with a period of four in response to a series of flashes (*41*, *62*, *71*−*73*), exhibiting "miss" parameters of 12−13% (*71*, *72*). Similar "miss" parameters (7−12%) have been estimated previously in PSII preparations on the basis of

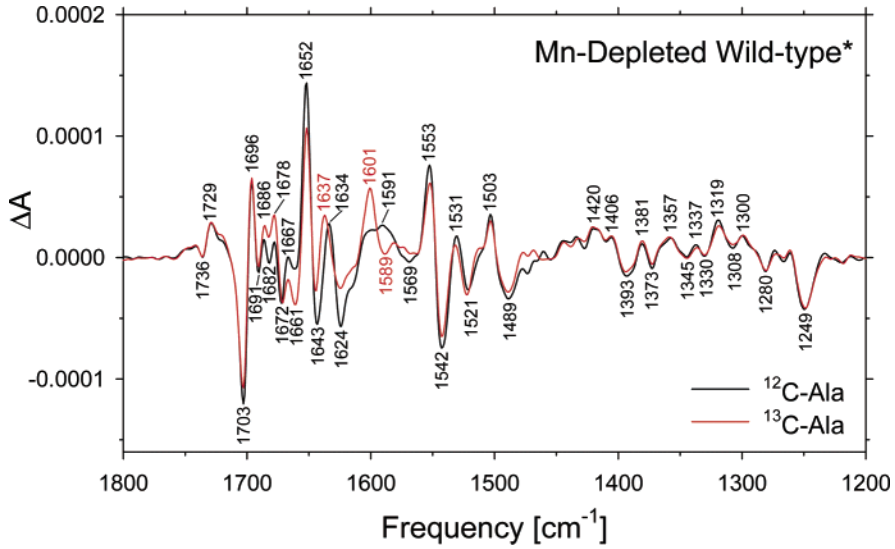

FIGURE 4: Comparison of the mid-frequency (1800−1200 cm^{-1}) flash-induced "light-*minus*-dark" FTIR difference spectra of Mn-depleted wild-type* PSII particles prepared from cells propagated in the presence of unlabeled (^{12}C) L-alanine (black line) or L-[1-^{13}C]alanine (red line). The spectra of the unlabeled and L-[1-^{13}C]alanine-labeled PSII particles represent the averages of twelve and 10 difference spectra, respectively. The spectra have been normalized to maximize their overlap between 1450 and 1200 cm^{-1}. Both spectra were collected under the same conditions as those shown in Figure 2 (e.g., with a sample temperature of 250 K and a resolution of 4 cm^{-1}).

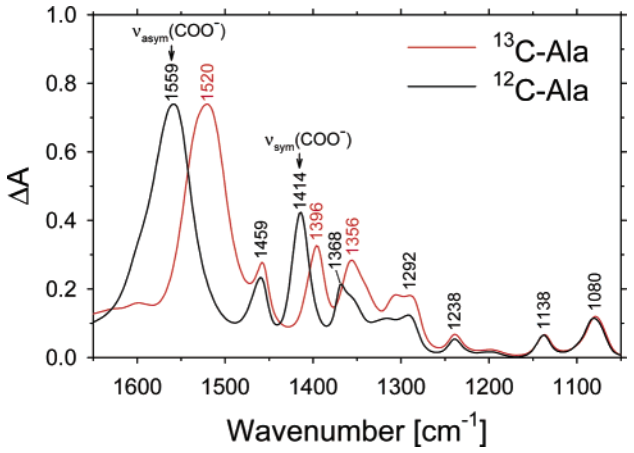

FIGURE 5: Absolute absorption spectra (1650−1050 cm^{-1}) of 2.5 mM unlabeled (^{12}C) L-alanine (black line) and 2.5 mM L-[1-^{13}C]-alanine (red line) dissolved in 3 M NaOH. The spectra have been normalized to their maximum amplitudes and the water band at 1657 cm^{-1} has been removed for clarity.

measurements of flash-induced period-four oscillations in the amplitudes of O_2 evolution (*81*, *82*), the S_2 state multiline EPR signal (*19*, *83*), electric field-induced charge recombination luminescence (*84*) and chlorophyll fluorescence yields (*85*). Finally, the features of the S_2-*minus*-S_1 difference spectrum are eliminated in the absence of the $(Mn)_4$ cluster, as shown by the light-*minus*-dark difference spectra of Mn-depleted PSII preparations that have been illuminated under the same experimental conditions as intact PSII preparations (Figure 4 and refs *64* and *66*). There can be little doubt, if any, that the features that are observed in the mid-frequency S_2-*minus*-S_1 FTIR difference spectrum of the unlabeled wild-type* PSII particles (Figures 1 and 2A) reflect protein structural changes that are associated with the $S_1 \rightarrow S_2$ transition.[2]

Symmetric Carboxylate Stretching Modes (1450−1300 cm^{-1}). A number of carboxylate modes appear in this region of the S_2-*minus*-S_1 FTIR difference spectrum (for reviews, see refs *35* and *36*), but the incorporation of L-[1-^{13}C]alanine altered the wild-type* spectrum only between 1360 and 1260 cm^{-1} (Figure 2A). The ^{12}C-*minus*-^{13}C double difference spectrum of this region (Figure 3) shows that the alterations appear to represent the shift of a single mode in both the S_1 and S_2 states. In the S_1 state, this mode appears at ∼1356 cm^{-1} and shifts to either ∼1339 or ∼1320 cm^{-1}. In the S_2 state, this mode appears at either ∼1339 or ∼1320 cm^{-1} and shifts to ∼1302 cm^{-1}. A shift of ∼17 cm^{-1} would be consistent with the ∼18 cm^{-1} shift of the symmetric carboxylate mode of alanine that is observed in L-[1-^{13}C]-alanine in solution (Figure 5). However, if the carboxylate group is a unidentate ligand of a metal ion (see below), the symmetric and asymmetric carboxylate stretching modes would be partly decoupled and the metal-ligating C−O group would acquire more single bond character (*92*, *93*). Treating

[2] A completely different S_2-*minus*-S_1 FTIR difference spectrum of wild-type PSII particles has been reported by one laboratory (e.g., refs *86*−*89*). This spectrum has almost no bands in common with the spectra that have been published by all other laboratories and is characterized by extremely broad features that are *unchanged* when the $(Mn)_4$ cluster is destroyed with the reductant hydroxylamine unless the samples are analyzed in the presence of excess EDTA (*87*). In contrast, we and others have observed that destroying the $(Mn)_4$ cluster with hydroxylamine completely abolishes the characteristic features of the S_2-*minus*-S_1 FTIR difference spectrum, whether EDTA is present (ref *64* and Figure 4) or not (ref *43* and unpublished). Recently, the spectrum that was reported in refs *86*−*89* was claimed to reflect an alternate structural form of the S_1 state that is produced when samples are dark-adapted at 4 °C for ≥ 2 h (*90*). However, other laboratories have observed that the features of the S_2-*minus*-S_1 FTIR difference spectrum are the same whether samples are dark adapted at 0−10 °C for 10 min (e.g., refs *43* and *71*) or 24 h (e.g., refs *37* and *39*). Furthermore, although the authors of ref *90* argue that the features in their recent spectra of long-term (2 h) dark-adapted samples correspond to the features in their previous spectra (e.g., those that are presented in refs *86*−*89*), *actually there is very little resemblance between these spectra* (e.g., compare Figure 4A of ref *90* with Figure 1A of ref *87*). The wild-type, mutant, and isotopically labeled "S_2-*minus*-S_1" FTIR difference spectra that are presented in refs *86*−*89* are undoubtedly dominated by artifacts, probably caused by increasing the glycerol concentration from 25% to ∼75% (*91*) during partial sample dehydration. In addition, the spectra may contain heating artifacts that are caused by recording "S_2" spectra during prolonged sample illumination rather than after brief illumination (*63*).

the C−O group that is vibrating at ∼1356 cm^{-1} as an isolated simple harmonic oscillator, ^{13}C-labeling will cause a downshift of 30 cm^{-1} (e.g., see ref *34*). However, for a real unidentate metal ligand, the symmetric and asymmetric carboxylate stretching modes are unlikely to be completely decoupled and, additionally, both modes may couple with other vibrations. Consequently, the actual L-[1-^{13}C]alanine-induced shift cannot be determined accurately. Indeed, global ^{13}C-labeling of PSII particles causes symmetric carboxylate stretching modes to shift by 18−42 cm^{-1} (*41*, *42*). Therefore, on the basis of these considerations, it is not possible to reliably determine if the L-[1-^{13}C]alanine-sensitive S_2 state mode appears at ∼1339 or ∼1320 cm^{-1} in unlabeled PSII particles.

Amide III modes from alanine-derived peptide groups could also appear in the symmetric carboxylate stretching region (*34*). However, we can exclude the possibility that the shifted bands correspond to such modes because amide III modes consist predominantly of N−H bending and C−N stretching vibrations (*34*, *94*) and global ^{15}N-labeling of PSII preparations causes no significant shifts in this region of the spectrum (*37*, *41*, *42*).

The incorporation of L-[1-^{13}C]alanine into the D1-A344G and D1-A344S PSII particles caused no significant alteration of any symmetric carboxylate stretching modes, as shown by the absence of significant L-[1-^{13}C]alanine-induced shifts in this region of the S_2-*minus*-S_1 FTIR difference spectra of the mutant PSII particles (Figure 2B,C) and by the absence of the ∼1356, ∼1339, ∼1320, and ∼1302 cm^{-1} bands from the ^{12}C-*minus*-^{13}C double difference spectra of the mutant PSII particles (blue and red lines in Figure 3). Because the only carboxylate group that will be labeled in the wild-type* PSII particles but not in the mutant PSII particles is the C-terminal α-COO^- group of the D1 polypeptide, the altered symmetric carboxylate stretching modes must correspond to the α-COO^- group of D1-Ala344. We conclude that the α-COO^- group of D1-Ala344 is structurally coupled to the $(Mn)_4$ cluster, with its $\nu_{sym}(COO^-)$ mode appearing at ∼1356 cm^{-1} in the S_1 state and at ∼1339 or ∼1320 cm^{-1} in the S_2 state.

Asymmetric Carboxylate Stretching Modes (1640−1500 cm^{-1}). Because the symmetric carboxylate stretching mode of D1-Ala344 appears in the S_2-*minus*-S_1 FTIR difference spectrum of wild-type* PSII particles (see previous section), the asymmetric carboxylate stretching mode should appear also. Indeed, the $\nu_{asym}(COO^-)$ mode of alanine in solution is more intense than the $\nu_{sym}(COO^-)$ mode and shifts to a greater extent in L-[1-^{13}C]alanine (∼39 vs ∼18 cm^{-1}, see Figure 5). Nevertheless, we are unable to unambiguously identify the $\nu_{asym}(COO^-)$ mode in either the S_1 state or the S_2 state. The incorporation of L-[1-^{13}C]alanine appears to have shifted numerous bands in the overlapping amide I/asymmetric carboxylate stretching regions of both the wild-type* and the mutant spectra (Figure 2). However, the spectral changes in these regions are complex and difficult to interpret, presumably because numerous bands overlap. The ^{12}C-*minus*-^{13}C double difference spectra of these regions (not shown) provided no meaningful insight. Nevertheless, we *can* conclude that no vibrational modes between ∼1556 and ∼1400 cm^{-1} in the unlabeled wild-type* spectrum were shifted by as much as ∼39 cm^{-1} after the incorporation of L-[1-^{13}C]alanine (Figure 2A). Consequently, the $\nu_{asym}(COO^-)$ mode of the α-COO^- group of D1-Ala344 must appear at a frequency >1556 cm^{-1} in both the S_1 and S_2 states.

Amide I (1690−1620 cm^{-1}) and Amide II (1570−1550 cm^{-1}) Modes. Because no symmetric carboxylate stretching modes were shifted by the incorporation of L-[1-^{13}C]alanine into the mutant PSII particles, the features that are observed to shift in the S_2-*minus*-S_1 difference spectra of the mutant PSII particles must correspond to amide I [predominantly C═O stretching (*34*, *94*)] and amide II [a mixture of N−H bending and C−N stretching (*34*, *94*)] modes from one or more alanine-derived peptide groups. The amide I modes should shift by 35−55 cm^{-1} in response to ^{13}C-labeling (*41*, *42*, *95*−*97*). Perhaps the ∼1651 and ∼1599 cm^{-1} features that are observed in the spectra of the wild-type* and mutant PSII particles are related, with a ∼1651 cm^{-1} mode shifting to ∼1599 cm^{-1} after the incorporation of L-[1-^{13}C]alanine. One possibility is that this mode corresponds to an alanine-derived peptide carbonyl group that is structurally coupled to the $(Mn)_4$ cluster. However, because remarkably similar alterations in modes near ∼1652 and ∼1601 cm^{-1} were observed in the light-*minus*-dark FTIR difference spectrum of Mn-depleted wild-type* PSII particles after the incorporation L-[1-^{13}C]alanine (Figure 4), it seems more likely that this mode occurs in a residual population of PSII reaction centers that lost the $(Mn)_4$ cluster during the purification of the PSII particles. To differentiate between these possibilities, we first must identify the features that are present in the light-*minus*-dark FTIR difference spectrum of the Mn-depleted wild-type* PSII particles.

The Flash-Induced Formation of $Y_D^\bullet$ at 250 K. The light-*minus*-dark FTIR difference spectrum of the unlabeled Mn-depleted wild-type* PSII particles (Figure 4) does not resemble the spectra of $Chl_Z^\bullet$-*minus*-Chl_Z (*98*), $Car^\bullet$-*minus*-Car (*99*), $Y_Z^\bullet$-*minus*-Y_Z (*100*), or $Q_A^{\bullet-}$-*minus*-Q_A (*74*, *101*−*104*). But then, neither $Chl_Z^\bullet$ nor $Car^\bullet$ would be expected to form at 250 K (*105*−*107*) and the 10 s delay between the laser flash and the commencement of data acquisition should have been sufficient for the decay of $Y_Z^\bullet$ and $Q_A^{\bullet-}$ (*44*, *63*, *64*). The spectrum also does not resemble those of the non-heme iron (Fe^{2+}-*minus*-Fe^{3+}) (*77*, *108*−*110*) or cyt b_{559}^{ox}-*minus* cyt b_{559}^{red} (*111*). Instead, the spectrum appears to be *identical* to the spectrum of $Y_D^\bullet$-*minus*-Y_D in *Synechocystis* sp. PCC 6803 (*43*, *112*).[3] All of the major bands that are shown in Figure 4 correspond to those that are in the published $Y_D^\bullet$-*minus*-Y_D spectra of *Synechocystis* 6803 within 1−3 cm^{-1} (e.g., compare Figure 4 with Figure 4 of ref *43* and with Figure 1A of ref *112*). The only significant difference is that the two small positive features that are observed at 1686 and 1678 cm^{-1} in Figure 4 appear as a single broad feature at ∼1684 cm^{-1} in the spectrum that is presented in ref *112* and as a barely resolved doublet in the spectrum that is presented in ref *43*.

The flash-induced formation of $Y_D^\bullet$ at 250 K in the Mn-depleted wild-type* PSII particles would not be unexpected. In Mn-depleted *Synechocystis* PSII particles, $Y_D^\bullet$ decays with a half-time of ∼7 min (*116*) to ∼30 min (*12*). Our samples were dark-adapted for longer periods than this. The flash-induced formation of $Y_D^\bullet$ at 250 K has been observed previously in Mn-depleted *Synechocystis* (*43*) and spinach (*77*) PSII particles with FTIR difference spectroscopy. The flash-induced formation of $Y_D^\bullet$ at 4 °C in Mn-depleted

spinach PSII preparations was reported in another FTIR study (*102*). More recent work has shown that Y_D is rapidly oxidized by $P_{680}^{\bullet+}$ in PSII preparations lacking the $(Mn)_4$ cluster (*12*) and that this reaction occurs at temperatures as low as 15 K (*117*) and 1.8 K (*118*). In contrast, the efficiency of $Y_Z^{\bullet}$ formation in Mn-depleted PSII preparations diminishes sharply below ~230 K (*119*−*121*).

We conclude that the light-*minus*-dark FTIR difference spectrum of Mn-depleted PSII particles (Figure 4) is that of $Y_D^{\bullet}$-*minus*-Y_D. Because the symmetric carboxylate stretching regions of the unlabeled and L-[1-^{13}C]alanine-labeled spectra are essentially identical, the L-[1-^{13}C]alanine-sensitive modes that are observed in this spectrum must correspond to one or more alanine-derived peptide carbonyl groups. One possibility is that an alanine-derived peptide carbonyl group is located in the vicinity of Y_D. However, in the secondary structure elements of peptides and proteins, peptide carbonyl groups are usually vibrationally coupled (*34*, *94*). Consequently, the alanine-derived peptide carbonyl group(s) that is(are) sensitive to L-[1-^{13}C]alanine-labeling in the $Y_D^{\bullet}$-*minus*-Y_D FTIR difference spectrum may not interact directly with Y_D.

Possible Ligation of Mn. The symmetric carboxylate mode [$\nu_{sym}(COO^-)$] of free ionic carboxylate groups appears near 1400 cm^{-1} [e.g., near 1414 cm^{-1} for acetates (*122*−*124*), near 1412 cm^{-1} for the α-COO$^-$ groups of free amino acids (*125*), and near 1402−1404 cm^{-1} for the side chains of Glu and Asp (*34*, *125*, *126*)]. For alanine in the solid state or in ^2H_2O, the $\nu_{sym}(COO^-)$ mode has been reported to appear at 1409−1418 cm^{-1} (*67*−*70*). We observed this mode at 1414 cm^{-1} for alanine in ^1H_2O (Figure 5). However, the $\nu_{sym}(COO^-)$ mode of the α-COO$^-$ group of D1-Ala344 appears at much lower frequency, at ~1356 cm^{-1} in the S_1 state and at ~1339 or ~1320 cm^{-1} in the S_2 state (Figure 3). These are downshifts of ~58 cm^{-1} in the S_1 state and either ~75 or ~94 cm^{-1} in the S_2 state compared to the position of this mode in alanine in solution.

The asymmetric carboxylate mode [$\nu_{asym}(COO^-)$] of free ionic carboxylate groups appears between 1550 and 1600 cm^{-1} [e.g., between 1553 and 1578 cm^{-1} for acetates (*122*−*124*), near 1598 cm^{-1} for the α-COO$^-$ groups of free amino acids (*125*, *127*), near 1582 cm^{-1} for the C-terminal α-COO$^-$ groups of peptides (*127*), and between 1556 and 1579 cm^{-1} for the side chains of Glu and Asp (*34*, *125*−*127*)]. For alanine in the solid state or in ^2H_2O, the $\nu_{asym}(COO^-)$ mode has been reported to appear at 1596−1623 cm^{-1} (*67*−*70*). We observed this mode at 1559 cm^{-1} for alanine in ^1H_2O (Figure 5). As discussed above, the $\nu_{asym}(COO^-)$ mode of the α-COO$^-$ group of D1-Ala344 must appear at frequencies > 1556 cm^{-1} in both the S_1 and S_2 states. Therefore, the difference in frequency, $\Delta\nu$, between the $\nu_{asym}(COO^-)$ and $\nu_{sym}(COO^-)$ modes of this α-COO$^-$ group must be >200 cm^{-1} in both the S_1 and S_2 states.

In metal-carboxylate complexes, the frequencies of the $\nu_{asym}(COO^-)$ and $\nu_{sym}(COO^-)$ modes and the difference in frequency between them, $\Delta\nu$, vary significantly with the metal ion and the type of carboxylate coordination (*92*, *122*−*124*). On the basis of examinations of a wide variety of metal-acetate and metal-trifluoroacetate complexes of known structures, an empirical correlation between $\Delta\nu$ and the nature of metal-carboxylate coordination has been established (*122*−*124*) and is widely used. The values of $\Delta\nu$ descend in the order:

$$\Delta\nu_{\text{unidentate}} > \Delta\nu_{\text{bridging}} \approx \Delta\nu_{\text{free ionic}} > \Delta\nu_{\text{chelating (bidentate)}}$$

For unidentate ligation, $\Delta\nu$ > 200 cm^{-1}, the position of the $\nu_{sym}(COO^-)$ mode is generally shifted to a lower frequency than its value in free ionic carboxylates, and the position of the $\nu_{asym}(COO^-)$ mode is generally shifted to a higher frequency. The magnitudes of these shifts can range from less than 30 cm^{-1} to more than 100 cm^{-1}. For bidentate chelating coordination, $\Delta\nu$ < 100 cm^{-1} and the $\nu_{sym}(COO^-)$ and $\nu_{asym}(COO^-)$ modes generally shift in the opposite direction compared to the shifts that are associated with unidentate ligation. For bidentate bridging ligation, $\Delta\nu \approx$ 160 cm^{-1} and the $\nu_{sym}(COO^-)$ and $\nu_{asym}(COO^-)$ modes can shift in either direction. These empirical observations have been supported by ab initio molecular orbital calculations (*93*).

Because we find that the $\nu_{sym}(COO^-)$ mode of the α-COO$^-$ group of D1-Ala344 is downshifted by ~58 cm^{-1} in the S_1 state and by ~75 or ~94 cm^{-1} in the S_2 state, we propose that the α-COO$^-$ group of D1-Ala344 is a unidentate ligand of a metal ion in both the S_1 and S_2 states. Indeed, we know of no plausible mechanism that could downshift the $\nu_{sym}(COO^-)$ mode of the α-COO$^-$ group of D1-Ala344 in PSII by 58−94 cm^{-1} other than unidentate ligation of a metal ion[4] except for asymmetric bidentate chelation of a metal ion (*124*), where the two metal−oxygen distances are substantially different, a situation that does not seem to be very common. Our conclusion that $\Delta\nu$ must be larger than 200 cm^{-1} in both the S_1 and S_2 states (see above) is consistent with our proposal of unidentate metal ligation by the α-COO$^-$ group of D1-Ala344 in both the S_1 and S_2 states.[5]

If the α-COO$^-$ group of D1-Ala344 is a unidentate ligand of a metal ion, is the ligated metal ion Mn or Ca? If D1-Ala344 ligates a Ca ion, then removal of Ca should significantly perturb the $\nu_{sym}(COO^-)$ mode of D1-Ala344 in both the S_1 and S_2 states. However, the removal of Ca from PSII produces no major changes in the symmetric

[3] This $Y_D^{\bullet}$-*minus*-Y_D spectrum (*43*, *112*) has been criticized by one laboratory (*113*) on grounds that the authors of refs *43* and *112* included formate (or formate plus phosphate) in their sample buffers. The authors of ref *113* argue that phosphate and formate cause large scale structural perturbations in PSII and have presented a light-*minus*-dark FTIR difference spectrum that was obtained in the presence of formate and phosphate under conditions that *caused* such structural perturbations (*113*). These authors (*113*) state that this spectrum "...is similar to..." the spectrum that is presented in ref *112* and argue that this "similarity" (between a spectrum that is presented as being artifactual and the spectrum that is presented in ref *112*) invalidates the $Y_D^{\bullet}$-*minus*-Y_D spectrum that is presented in ref *112*. *However, there is actually no similarity between these two spectra* (compare Figure 4D of ref *113* with Figure 1A of ref *112*). Therefore, the criticisms that are raised by the authors of ref *113* (and that have been repeated in subsequent publications by this group) are without merit. Furthermore, our spectrum (Figure 4) was obtained in the absence of both phosphate and formate and closely resembles the spectra that are presented in refs *43* and *112*. Finally, isotopic labeling with L-[ring-4-^{13}C]tyrosine caused no unambiguous band shifts in the alternate $Y_D^{\bullet}$-*minus*-Y_D spectrum that was presented by the authors of ref *113* (see Figure 7D of ref *114*), whereas the incorporation of L-[ring-4-^{13}C]tyrosine clearly and unambiguously shifted two discrete bands in the $Y_D^{\bullet}$-*minus*-Y_D spectrum that was presented in refs *43* and *112*, a positive band at ~1503 cm^{-1} and a negative band at ~1250 cm^{-1}. These bands were assigned to the ν(CO) mode of $Y_D^{\bullet}$ and the δ(COH) mode of Y_D, respectively (*36*, *43*, *112*), assignments that have been supported by recent density functional calculations (*115*).

carboxylate stretching region of the S_2-*minus*-S_1 FTIR difference spectrum (*38*). Therefore, we propose that D1-Ala344 ligates a Mn ion in both the S_1 and S_2 states.

The magnitude of the downshift of the $\nu_{sym}(COO^-)$ mode between the S_1 and S_2 states ($\sim$17 or $\sim$36 cm^{-1}) is much too large to be explained by a nonspecific through-space electrostatic interaction between the α-COO^- moiety of D1-Ala344 and the $(Mn)_4$ cluster. In reaction centers from *Rhodobacter capsulatus*, the introduction of a negatively charged Asp residue $\sim$2.6 Å from the oxygen of the C_9-keto group of the photoactive accessory BChl molecule on the L subunit shifted the frequency of the $\nu C_9{=}O$ mode by only 7 cm^{-1} (*129*). The cause of this shift was attributed to a nonspecific charge-dipole interaction between the negatively charged Asp carboxyl group and the C_9-keto group of the BChl molecule. Therefore, to explain the much larger magnitude of the $\sim$17 or $\sim$36 cm^{-1} downshift of the $\nu_{sym}(COO^-)$ mode of D1-Ala344, we propose that the α-COO^- group of D1-Ala344 is a unidentate ligand of a Mn ion whose charge increases during the $S_1 \rightarrow S_2$ transition.

The concept of charge accumulation on the $(Mn)_4$ cluster has been advanced by many workers in the field who propose that, during the $S_1 \rightarrow S_2$ transition, the $(Mn)_4$ cluster acquires an uncompensated positive charge when a Mn(III) ion is oxidized to Mn(IV). Although this advance in oxidation state during the $S_1 \rightarrow S_2$ transition is almost universally accepted, the concept of an accompanying charge accumulation is not (*5*, *130*, *131*). Nevertheless, the basis for the belief that the $(Mn)_4$ cluster *does* acquire an uncompensated positive charge during the $S_1 \rightarrow S_2$ transition consists of (i) measurements of optical absorption changes that occur during the individual S state transitions and that have been attributed to electrochromic bandshifts (*132*−*137*), (ii) measurements of the extents of proton release during the individual S state transitions that correlate with the electrochromic bandshifts (*138*−*141*), (iii) measurements of the kinetics of $P_{680}^{\bullet+}$ reduction by Y_Z in the individual S states (*137*, *142*, *143*), and (iv) measurements of the temperature dependence of the kinetics of $P_{680}^{\bullet+}$ reduction in the individual S states (*144*). Accordingly, there is considerable evidence supporting charge accumulation on the $(Mn)_4$ cluster during the $S_1 \rightarrow S_2$ transition (*132*−*144*). We propose that this increased positive charge is sufficient to significantly downshift the $\nu_{sym}(COO^-)$ modes of one or more Mn-coordinating carboxylate groups in the S_2 state, including the α-COO^- group of D1-Ala344. The FTIR spectral changes that accompany the $S_1 \rightarrow S_2$ transition would be expected to reflect additional structural changes that result from the protein's response to this increased positive charge. Indeed, such changes may account for most, if not all, of the other band shifts that are observed in the S_2-*minus*-S_1 FTIR difference spectrum, including the distinctive shift of a $\nu_{sym}(COO^-)$ mode from $\sim$1402 to $\sim$1364 cm^{-1} that has been proposed to reflect a change in the coordination mode of a Mn-ligating carboxylate residue (*37*, *38*).

Another important question then becomes whether the oxidizing equivalent that is transferred to the $(Mn)_4$ cluster during the $S_1 \rightarrow S_2$ transition is localized (i.e., resides solely on the Mn(IV) ion that is produced during this transition) or delocalized (i.e., is shared between multiple Mn ions). Analyses of di-μ-oxo bridged Mn(III)Mn(IV) complexes with density functional theory show that partial charge delocalization occurs in these complexes (*145*−*148*), with the possibility that some electron density may be transferred from the dz^2 orbital of the Mn(III) ion to the nonbonding dx^2-y^2 orbital of the Mn(IV) ion (*146*, *147*). The extent of this partial delocalization is small but depends on the nature of the Mn ligands and whether the Mn_2O_2 core is planar or not (*147*). Consequently, it is possible that some partial charge delocalization may occur in the $(Mn)_4$ cluster in PSII. However, if the S_2 state consists of a single Mn(III) ion that interacts with three Mn(IV) ions (*2*, *3*, *14*−*16*), then the extent of this charge delocalization is likely to be quite small. Consequently, the extra oxidizing equivalent that is transferred to the $(Mn)_4$ cluster during the $S_1 \rightarrow S_2$ transition would probably reside primarily on the Mn(IV) ion that is produced during this transition.

On the basis of the considerations that are discussed the previous paragraph, we propose that D1-Ala344 is coordinated to the Mn ion that undergoes an oxidation during the $S_1 \rightarrow S_2$ transition. If the α-COO^- group of D1-Ala344 is a unidentate ligand of a Mn ion whose charge increases during the $S_1 \rightarrow S_2$ transition, the increase in charge would be expected to weaken the ligating C−O bond, thereby decreasing the frequency of the $\nu_{sym}(COO^-)$ mode. Although we know of little relevant literature on model compounds, the limited data available (e.g., Table 3−19 in ref *124*) suggest that our observed downshift of $\sim$17 or $\sim$36 cm^{-1} is consistent with an increase in charge on the metal ion that is ligated by the α-COO^- group of D1-Ala344. Therefore, if the extra oxidizing equivalent that is transferred to the $(Mn)_4$ cluster during the $S_1 \rightarrow S_2$ transition resides primarily on the Mn(IV) ion that is produced during this transition (as we expect), then our data are consistent with the α-COO^- group of Ala344 ligating the Mn ion that is oxidized during the $S_1 \rightarrow S_2$ transition.

[4] Two other possibilities can be discounted. First, the $\nu_{sym}(COO^-)$ mode is not downshifted because the α-COO^- group of D1-Ala344 is protonated. If this group was protonated, its ν(C−O) mode would appear between 1253 and 1120 cm^{-1} (*125*, *126*), not between 1356 and 1320 cm^{-1}. Furthermore, unless the C═O group was strongly hydrogen bonded, the ν(C═O) mode would appear between 1710 and 1790 cm^{-1} (*34*, *126*), whereas we observe no L-[1-^{13}C]alanine-induced shifts in this region of the spectrum (Figure 2A). Second, the $\nu_{sym}(COO^-)$ mode is not downshifted because of a strong hydrogen bond involving the α-COO^- group of D1-Ala344. If the downshift was caused by a hydrogen bonding interaction, the region of the FTIR difference spectrum between 1380 and 1280 cm^{-1} should be altered by exchanging ^2H_2O for ^1H_2O. However, overnight exchanges of ^2H_2O for ^1H_2O in spinach PSII preparations (*39*) and in *Thermosynechococcus elongatus* PSII particles (*73*) caused no significant changes in the S_2-*minus*-S_1 FTIR difference spectrum between 1400 and 1300 cm^{-1}. Furthermore, we know of no precedent for hydrogen bonding interactions shifting a symmetric carboxylate stretching mode by 58−94 cm^{-1}.

[5] The suitability of employing $\Delta\nu$ values to predict types of carboxylate coordination in PSII has been challenged on grounds that synthetic oxo-bridged dinuclear and trinuclear Mn complexes containing bidentate bridging carboxylate groups can have $\Delta\nu$ values ranging from $\sim$100 to > 200 cm^{-1} (*128*). However, in all of the complexes that were examined in ref *128*, the $\nu_{sym}(COO^-)$ modes appeared between 1410 and 1450 cm^{-1}, similar to or larger than the frequency of the $\nu_{sym}(COO^-)$ modes of free ionic carboxylates. Consequently, for none of the complexes examined in ref *128* would unidentate ligation have been predicted. In our analyses, we have emphasized the absolute frequencies of the $\nu_{sym}(COO^-)$ modes rather than the $\Delta\nu$ values. Values of $\nu_{sym}(COO^-)$ that are significantly lower than the values of $\nu_{sym}(COO^-)$ in free ionic carboxylates are uniquely associated with unidentate ligation except in the uncommon case of asymmetric bidentate chelation of a metal ion (*124*), where the two metal−oxygen distances are substantially different.

CONCLUDING REMARKS

The $\nu_{sym}(COO^-)$ mode of the α-COO^- group of D1-Ala344 is clearly present in the flash-induced S_2-*minus*-S_1 FTIR difference spectrum of wild-type* PSII particles. This result shows that the C-terminal carboxylate of the D1 polypeptide is structurally coupled to the $(Mn)_4$ cluster. The frequencies of the $\nu_{sym}(COO^-)$ mode of the α-COO^- group of D1-Ala344 in the S_1 and S_2 states are substantially downshifted (by ∼58 cm^{-1} in the S_1 state and by ∼75 or ∼94 cm^{-1} in the S_2 state) from the position of the $\nu_{sym}(COO^-)$ mode of alanine in solution. These substantial downshifts are consistent with unidentate ligation of the $(Mn)_4$ cluster by the α-COO^- group of D1-Ala344 in both the S_1 and S_2 states. The $\nu_{sym}(COO^-)$ mode of the α-COO^- group of D1-Ala344 downshifts by ∼17 or ∼36 cm^{-1} during the $S_1 \rightarrow S_2$ transition. The magnitude of this shift is consistent with the α-COO^- group of D1-Ala344 ligating a Mn ion whose charge increases during the $S_1 \rightarrow S_2$ transition. Accordingly, we propose that the α-COO^- group of D1-Ala344 ligates the Mn ion that undergoes an oxidation during this transition. Finally, control experiments that were conducted with Mn-depleted PSII particles show that tyrosine Y_D may be structurally coupled to the carbonyl oxygen of an alanine-derived peptide carbonyl group.

ACKNOWLEDGMENT

We are grateful to Anh P. Nguyen for maintaining the wild-type* and mutant cultures of *Synechocystis* sp. PCC 6803 and for isolating the thylakoid membranes that were used for purifying the PSII particles. We are indebted to Jörg Schwender for performing the mass spectrometry analyses, to David F. Bocian for helping interpret the FTIR data, to Takumi Noguchi, Catherine Berthomieu, Jacques Breton, and Eliane Nabedryk for the enlightening discussions, and to Takumi Noguchi and the reviewers for helpful comments on the manuscript.

REFERENCES

1. Britt, R. D. (1996) Oxygen Evolution in *Oxygenic Photosynthesis: The Light Reactions* (Ort, D. R., and Yocum, C. F., Eds.) pp 137−164, Kluwer Academic Publishers, Dordrecht, The Netherlands.
2. Yachandra, V. K., Sauer, K., and Klein, M. P. (1996) Manganese Cluster in Photosynthesis: Where Plants Oxidize Water to Dioxygen. *Chem. Rev. 96*, 2927−2950.
3. Penner-Hahn, J. E. (1998) Structural Characterization of the Mn Site in the Photosynthetic Oxygen-Evolving Complex. *Struct. Bonding 90*, 1−36.
4. Debus, R. J. (2000) The Polypeptides of Photosystem II and Their Influence on Mangano-Tyrosyl Based Oxygen Evolution in *Metal Ions in Biological Systems, Vol. 37, Manganese and Its Role in Biological Processes* (Sigel, A., and Sigel, H., Eds.) pp 657−711, Marcel Dekker, New York.
5. Tommos, C., and Babcock, G. T. (2000) Proton and Hydrogen Currents in Photosynthetic Water Oxidation. *Biochim. Biophys. Acta 1458*, 199−219.
6. Pecoraro, V. L., and Hsieh, W.-Y. (2000) The Use of Model Complexes to Elucidate the Structure and Function of Manganese Redox Enzymes in *Metal Ions in Biological Systems, Vol. 37, Manganese and Its Role in Biological Processes* (Sigel, A., and Sigel, H., Eds.) pp 429−504, Marcel Dekker, Inc., New York.
7. Renger, G. (2001) Photosynthetic Water Oxidation to Molecular Oxygen: Apparatus and Mechanism. *Biochim. Biophys. Acta 1503*, 210−228.
8. Diner, B. A., and Rappaport, F. (2002) Structure, Dynamics, and Energetics of the Primary Photochemistry of Photosystem II of Oxygenic Photosynthesis. *Annu. Rev. Plant Biol. 53*, 551−580.
9. Goussias, C., Boussac, A., and Rutherford, A. W. (2002) Photosystem II and Photosynthetic Oxidation of Water: An Overview. *Philos. Trans. R. Soc. London, Ser. B 357*, 1369−1381.
10. Cinco, R. M., Holman, K. L., Robblee, J. H., Yano, J., Pizarro, S. A., Bellacchio, E., Sauer, K., and Yachandra, V. K. (2002) Calcium EXAFS Establishes the Mn−Ca Cluster in the Oxygen-Evolving Complex of Photosystem II. *Biochemistry 41*, 12928−12933.
11. Clemens, K. L., Force, D. A., and Britt, R. D. (2002) Acetate Binding at the Photosystem II Oxygen Evolving Complex: An S_2-state Multiline Signal ESEEM Study. *J. Am. Chem. Soc. 124*, 10921−10933.
12. Faller, P., Debus, R. J., Brettel, K., Sugiura, M., Rutherford, A. W., and Boussac, A. (2001) Rapid Formation of the Stable Tyrosyl Radical in Photosystem II. *Proc. Natl. Acad. Sci. U.S.A. 98*, 14368−14373.
13. Ananyev, G. A., Sakiyan, I., Diner, B. A., and Dismukes, G. C. (2002) A Functional Role for Tyrosine-D in Assembly of the Inorganic Core of the Water Oxidase Complex of Photosystem II and the Kinetics of Water Oxidation. *Biochemistry 41*, 974−980.
14. Robblee, J. H., Cinco, R. M., and Yachandra, V. K. (2001) X-ray Spectroscopy-Based Structure of the Mn Cluster and Mechanism of Photosynthetic Oxygen Evolution. *Biochim. Biophys. Acta 1503*, 7−23.
15. Dau, H., Iuzzolino, L., and Dittmer, J. (2001) The Tetra-Manganese Complex of Photosystem II during its Redox Cycle − X-ray Absorption Results and Mechanistic Implications. *Biochim. Biophys. Acta 1503*, 24−39.
16. Yachandra, V. K. (2002) Structure of the Manganese Complex in Photosystem II: Insights from X-ray Spectroscopy. *Philos. Trans. R. Soc. London, Ser. B 357*, 1347−1358.
17. Zheng, M., and Dismukes, G. C. (1996) Orbital Configuration of the Valence Electrons, Ligand Field Symmetry, and Manganese Oxidation State of the Photosynthetic Water Oxidizing Complex: Analysis of the S_2 State Multiline EPR Signals. *Inorg. Chem. 35*, 3307−3319.
18. Carrell, T. G., Tyryshkin, A. M., and Dismukes, G. C. (2002) An Evaluation of Structural Models for the Photosynthetic Water-Oxidizing Complex Derived from Spectroscopic and X-ray Diffraction Signatures. *J. Biol. Inorg. Chem. 7*, 2−22.
19. Messinger, J., Robblee, J. H., Bergmann, U., Fernandez, C., Glatzel, P., Visser, H., Cinco, R. M., McFarlane, K. L., Bellacchio, E., Pizarro, S. A., Cramer, S. P., Sauer, K., Klein, M. P., and Yachandra, V. K. (2001) Absence of Mn-Centered Oxidation in the $S_2 \rightarrow S_3$ Transition: Implications for the Mechanism of Photosynthetic Water Oxidation. *J. Am. Chem. Soc. 123*, 7804−7820.
20. Zouni, A., Witt, H. T., Kern, J., Fromme, P., Krauss, N., Saenger, W., and Orth, P. (2001) Crystal Structure of Photosystem II from *Synechococcus elongatus* at 3.8 Å Resolution. *Nature 409*, 739−743.
21. Fromme, P., Kern, J., Loll, B., Biesiadka, J., Saenger, W., Witt, H. T., Krauss, N., and Zouni, A. (2002) Functional Implication on the Mechanism of the Function of Photosystem II Including Water Oxidation base on the Structure of Photosystem II. *Philos. Trans. R. Soc. London, Ser. B 357*, 1337−1345.
22. Kamiya, N., and Shen, J.-R. (2003) Crystal Structure of Oxygen-Evolving Photosystem II from *Thermosynechococcus vulcanus* at 3.7 Å Resolution. *Proc. Natl. Acad. Sci. U.S.A. 100*, 98−103.
23. Peloquin, J. M., Campbell, K. A., Randall, D. W., Evanchik, M. A., Pecoraro, V. L., Armstrong, W. H., and Britt, R. D. (2000) ^{55}Mn ENDOR of the S_2-state Multiline EPR Signal of Photosystem II: Implications on the Structure of the Tetranuclear Mn Cluster. *J. Am. Chem. Soc. 122*, 10926−10942.
24. Peloquin, J. M., and Britt, R. D. (2001) EPR/ENDOR Characterization of the Physical and Electronic Structure of the OEC Mn Cluster. *Biochim. Biophys. Acta 1503*, 96−111.
25. Diner, B. A. (2001) Amino Acid Residues Involved in the Coordination and Assembly of the Manganese Cluster of Photosystem II: Proton-Coupled Electron Transport of the Redox-Active Tyrosines and Its Relationship to Water Oxidation. *Biochim. Biophys. Acta 1503*, 147−163.
26. Debus, R. J. (2001) Amino Acid Residues that Modulate the Properties of Tyrosine Y_Z and the Manganese Cluster in the Water Oxidizing Complex of Photosystem II. *Biochim. Biophys. Acta 1503*, 164−186.
27. Debus, R. J. (2004) The O_2 Evolving Site as Analyzed by Site-Directed Mutagenesis in *The Water/Plastoquinone Oxido-Reduc-*

tase of Photosynthesis (Wydrzynski, T., and Satoh, Ki., Eds.) Kluwer Academic Publishers, Dordrecht, The Netherlands, in press.
28. Debus, R. J., Campbell, K. A., Gregor, W., Li, Z.-L., Burnap, R. L., and Britt, R. D. (2001) Does Histidine 332 of the D1 Polypeptide Ligate the Manganese Cluster in Photosystem II? An Electron Spin−Echo Envelope Modulation Study. *Biochemistry 40*, 3690−3699.
29. Debus, R. J., Aznar, C., Campbell, K. A., Gregor, W., Diner, B. A., and Britt, R. D. (2003) Does Aspartate 170 of the D1 Polypeptide Ligate the Manganese Cluster in Photosystem II? An EPR and ESEEM Study. *Biochemistry 42*, 10600−10608.
30. Chu, H.-A., Debus, R. J., and Babcock, G. T. (2001) D1-Asp170 is Structurally Coupled to the Oxygen Evolving Complex in Photosystem II as Revealed by Light-Induced Fourier Transform Infrared Difference Spectroscopy. *Biochemistry 40*, 2312−2316.
31. Mäntele, W. (1996) Infrared and Fourier Transform Infrared Spectroscopy in *Biophysical Techniques in Photosynthesis* (Amesz, J., and Hoff, A. J., Eds.) pp 137−160, Kluwer Academic Publishers, Dordrecht, The Netherlands.
32. Vogel, R., and Siebert, F. (2000) Vibrational Spectroscopy as a Tool for Probing Protein Function. *Curr. Opin. Chem. Biol. 4*, 518−523.
33. Zscherp, C., and Barth, A. (2001) Reaction-Induced Infrared Difference Spectroscopy for the Study of Protein Reaction Mechanisms. *Biochemistry 40*, 1875−1883.
34. Barth, A., and Zscherp, C. (2002) What Vibrations Tell Us About Proteins. *Q. Rev. Biophys. 35*, 369−430.
35. Chu, H.-A., Hillier, W., Law, N. A., and Babcock, G. T. (2001) Vibrational Spectroscopy of the Oxygen-Evolving Complex and of Manganese Model Compounds. *Biochim. Biophys. Acta 1503*, 69−82.
36. Noguchi, T., and Berthomieu, C. (2004) Molecular Analysis by Vibrational Spectroscopy in *Photosystem II: The Water/Plastoquinone Oxido-Reductase of Photosynthesis* (Wydrzynski, T., and Satoh, Ki., Eds.) Kluwer Academic Publishers, Dordrecht, The Netherlands, in press.
37. Noguchi, T., Ono, T.-A., and Inoue, Y. (1995) Direct Detection of a Carboxylate Bridge Between Mn and Ca^{2+} in the Photosynthetic Oxygen-Evolving Center by Means of Fourier Transform Infrared Spectroscopy. *Biochim. Biophys. Acta 1228*, 189−200.
38. Kimura, Y., and Ono, T.-A. (2001) Chelator-Induced Disappearance of Carboxylate Stretching Vibrational Modes in S_2/S_1 FTIR Spectrum in Oxygen-Evolving Complex of Photosystem II. *Biochemistry 40*, 14061−14068.
39. Noguchi, T., Ono, T.-A., and Inoue, Y. (1995) A Carboxylate Ligand Interacting with Water in the Oxygen-Evolving Center of Photosystem II as Revealed by Fourier Transform Infrared Spectroscopy. *Biochim. Biophys. Acta 1232*, 59−66.
40. Noguchi, T., Sugiura, M., and Inoue, Y. (1999) FTIR Studies on the Amino-Acid Ligands of the Photosynthetic Oxygen-Evolving Mn-Cluster in *Fourier Transform Spectroscopy: Twelfth International Conference* (Itoh, K., and Tasumi, M., Eds.) pp 459−460, Waseda University Press, Tokyo, Japan.
41. Noguchi, T., and Sugiura, M. (2003) Analysis of Flash-Induced FTIR Difference Spectra of the S-state cycle in the Photosynthetic Water-Oxidizing Complex by Uniform ^{15}N and ^{13}C isotope Labeling. *Biochemistry 42*, 6035−6042.
42. Kimura, Y., Mizusawa, N., Ishii, A., Yamanari, T., and Ono, T.-A. (2003) Changes of Low-Frequency Vibrational Modes Induced by Universal ^{15}N- and ^{13}C-Isotope Labeling in S_2/S_1 FTIR Difference Spectrum of Oxygen-Evolving Complex. *Biochemistry 42*, 13170−13177.
43. Noguchi, T., Inoue, Y., and Tang, X. S. (1997) Structural Coupling between the Oxygen-Evolving Mn Cluster and a Tyrosine Residue in Photosystem II as Revealed by Fourier Transform Infrared Spectroscopy. *Biochemistry 36*, 14705−14711.
44. Noguchi, T., Inoue, Y., and Tang, X.-S. (1999) Structure of a Histidine Ligand in the Photosynthetic Oxygen-Evolving Complex as Studied by Light-Induced Fourier Transform Infrared Spectroscopy. *Biochemistry 38*, 10187−10195.
45. Nixon, P. J., Trost, J. T., and Diner, B. A. (1992) Role of the Carboxy Terminus of Polypeptide D1 in the Assembly of a Functional Water-Oxidizing Manganese Cluster in Photosystem II of the Cyanobacterium *Synechocystis* sp. PCC 6803: Assembly Requires a Free Carboxyl Group at *C*-Terminal Position 344. *Biochemistry 31*, 10859−10871.
46. Kashino, Y., Lauber, W. M., Carroll, J. A., Wang, Q. J., Whitmarsh, J., Satoh, Ka., and Pakrasi, H. B. (2002) Proteomic analysis of a highly active photosystem II preparation from the cyanobacterium *Synechocystis* sp PCC 6803 reveals the presence of novel polypeptides. *Biochemistry 41*, 8004−8012.
47. Kaneko, T., Sato, S., Kotani, H., Tanaka, A., Asamizu, E., Nakamura, Y., Miyajima, N., Hirosawa, M., Sugiura, M., Sasamoto, S., Kimura, T., Hosouchi, T., Matsuno, A., Muraki, A., Nakazaki, N., Naruo, K., Okamura, S., Shimpo, S., Takeuchi, C., Wada, T., Watanabe, A., Yamada, M., Yasuda, M., and Tabata, S. (1996) Sequence Analysis of the Genome of the Unicellular Cyanobacterium *Synechocystis* sp. Strain PCC 6803. II. Sequence Determination of the Entire Genome and Assignment of Potential Protein-Coding Regions. *DNA Res. 3*, 109−136, Suppl. 185−209.
48. Ikeuchi, M., and Tabata, S. (2001) *Synechocystis* sp. PCC 6803 − a Useful Tool in the Study of the Genetics of Cyanobacteria. *Photosynth. Res. 70*, 73−83.
49. Chu, H.-A., Babcock, G. T., and Debus, R. J. (2001) Possible Ligation of the Mn cluster in Photosystem II by the Carboxyl-Terminus of the D1 Polypeptide: An FTIR Study in *PS2001 Proceedings: 12th International Congress on Photosynthesis*, paper S13−P026, pp 1−4, CSIRO Publishing, Melbourne, Australia (published on the web: www.publish.csiro.au/PS2001).
50. Williams, J. G. K. (1988) Construction of Specific Mutations in Photosystem II Photosynthetic Reaction Center by Genetic Engineering Methods in *Synechocystis* 6803. *Methods Enzymol. 167*, 766−778.
51. Chu, H.-A., Nguyen, A. P., and Debus, R. J. (1994) Site-Directed Photosystem II Mutants with Perturbed Oxygen Evolving Properties. 2. Increased Binding or Photooxidation of Manganese in the Absence of the Extrinsic 33-kDa Polypeptide In Vivo. *Biochemistry 33*, 6150−6157.
52. Chu, H.-A., Nguyen, A. P., and Debus, R. J. (1995) Amino Acid Residues that Influence the Binding of Manganese or Calcium to Photosystem II. 2. The Carboxy-terminal Domain of the D1 Polypeptide. *Biochemistry 34*, 5859−5882.
53. Debus, R. J., Nguyen, A. P., and Conway, A. B. (1990) Identification of Ligands to Manganese and Calcium in Photosystem II by Site-Directed Mutagenesis in *Current Research in Photosynthesis* (Baltscheffsky, M., Ed.) Vol. I, pp 829−832, Kluwer Academic Publishers, Dordrecht, The Netherlands.
54. Chu, H.-A., Nguyen, A. P., and Debus, R. J. (1994) Site-Directed Photosystem II Mutants with Perturbed Oxygen Evolving Properties: 1. Instability or Inefficient Assembly of the Manganese Cluster *In Vivo*. *Biochemistry 33*, 6137−6149.
55. Rippka, R., Deruelles, J., Waterbury, J. B., Herdman, M., and Stanier, R. Y. (1979) Generic Assignments, Strain Histories and Properties of Pure Cultures of Cyanobacteria. *J. Gen. Microbiol. 111*, 1−61.
56. Peloquin, J. M., Tang, X.-S., Diner, B. A., and Britt, R. D. (1999) An Electron Spin−Echo Envelope Modulation (ESEEM) Study of the Q_A Binding Pocket of PSII Reaction Centers from Spinach and *Synechocystis*. *Biochemistry 38*, 2057−2067.
57. Hays, A.-M. A., Vassiliev, I. R., Golbeck, J. H., and Debus, R. J. (1998) Role of D1-His190 in Proton-Coupled Electron-Transfer Reactions in Photosystem II: A Chemical Complementation Study. *Biochemistry 37*, 11352−11365.
58. Peiffer, W. E., Ingle, R. T., and Ferguson-Miller, S. (1990) Structurally Unique Plant Cytochrome *c* Oxidase Isolated from Wheat Germ, a Rich Source of Plant Mitochondrial Enzyme. *Biochemistry 29*, 8696−8701.
59. Das Neves, H. J. C., and Vasconcelos, A. M. P. (1987) Capillary Gas Chromatography of Amino Acids, Including Asparagine and Glutamine: Sensitive Gas Chromatographic-Mass Spectrometric and Selected Ion Monitoring Gas Chromatographic-Mass Spectrometric Detection of the N,O(S)-*tert*-Butyldimethylsilyl Derivatives, *J. Chromatogr. 392*, 249−258.
60. Schwender, J., and Ohlrogge, J. B. (2002) Probing *In Vivo* Metabolism by Stable Isotope Labeling of Storage Lipids and Proteins in Developing *Brassica napus* Embryos. *Plant Physiol. 130*, 347−361.
61. Chu, H.-A., Gardner, M. T., Hillier, W., and Babcock, G. T. (2000) Low-Frequency Fourier Transform Infrared Spectroscopy of the Oxygen-Evolving Complexes in Photosystem II. *Photosyn. Res. 66*, 57−63.
62. Hillier, W., and Babcock, G. T. (2001) S-State Dependent FTIR Difference Spectra for the Photosystem II Oxygen Evolving Complex. *Biochemistry 40*, 1503−1509.
63. Onoda, K., Mino, H., Inoue, Y., and Noguchi, T. (2000) An FTIR Study on the Structure of the Oxygen-Evolving Mn-cluster of

Photosystem II in Different Spin Forms of the S_2 State. *Photosynth. Res. 63*, 47−57.
64. Noguchi, T., and Sugiura, M. (2000) Structure of an Active Water Molecule in the Water-Oxidizing Complex of Photosystem II as Studied by FTIR Sectroscopy. *Biochemistry 39*, 10943−10949.
65. Hatano-Iwasaki, A., Minagawa, J., Inoue, Y., and Takahashi, Y. (2001) Two Functionally Distinct Manganese Clusters formed by Introducing a Mutation in the Carboxyl Terminus of a Photosystem II Reaction Center Polypeptide, D1, of the Green Alga *Chlamydomonas reinhardtii*. *Biochim. Biophys. Acta 1504*, 299−310.
66. Chu, H.-A., Gardner, M. T., O'Brien, J. P., and Babcock, G. T. (1999) Low-frequency Fourier Transform Infrared Spectroscopy of the Oxygen-Evolving and Quinone Acceptor Complexes in Photosystem II. *Biochemistry 38*, 4533−4541.
67. Susi, H., and Byler, D. M. (1980) Vibrational Analysis of L-Alanine and Deuterated Analogs. *J. Mol. Struct. 63*, 1−11.
68. Diem, M., Polavarapu, P. L., Oboodi, M., and Nafie, L. A. (1982) Vibrational Circular Dichroism in Amino Acids and Peptides. 4. Vibrational Analysis, Assignments, and Solution-Phase Raman Spectra of Deuterated Isotopomers of Alanine. *J. Am. Chem. Soc. 104*, 3329−3336.
69. Diem, M. (1988) Infrared Vibrational Circular Dichrosim of Alanine in the Midinfrared Region: Isotopic Effects, *J. Am. Chem. Soc. 110*, 6967−6970.
70. Tortonda, F. R., Pascual-Ahuir, J.-L., Silla, E., Tunon, I., and Ramirez, F. (1998) Aminoacid Zwitterions in Solution: Geometric, Energetic, and Vibrational Analysis Using Density Functional Theory-Continuum Model Calculations. *J. Chem. Phys. 109*, 592−603.
71. Noguchi, T., and Sugiura, M. (2001) Flash-Induced Fourier Transform Infrared Detection of the Structural Changes during the S-State Cycle of the Oxygen-Evolving Complex in Photosystem II. *Biochemistry 40*, 1497−1502.
72. Noguchi, T., and Sugiura, M. (2002) Flash-Induced FTIR Difference Spectra of the Water Oxidizing Complex in Moderately Hydrated Photosystem II Core Films: Effect of Hydration Extent on S−State Transitions. *Biochemistry 41*, 2322−2330.
73. Noguchi, T., and Sugiura, M. (2002) FTIR Detection of Water Reactions During the Flash-Induced S-state cycle of the Photosynthetic Water-Oxidizing Complex. *Biochemistry 41*, 15706−15712.
74. Noguchi, T., Ono, T.-A., and Inoue, Y. (1992) Detection of Structural Changes upon S_1-to-S_2 Transition in the Oxygen-Evolving Manganese Cluster in Photosystem II by Light-Induced Fourier Transform Infrared Difference Spectroscopy. *Biochemistry 31*, 5953−5956.
75. Noguchi, T., Ono, T.-A., and Inoue, Y. (1993) Temperature Dependence of the $S_1 \rightarrow S_2$ Transition in the Oxygen-Evolving Complex of Photosystem II Studied by FT-IR Spectroscopy. *Biochim. Biophys. Acta 1143*, 333−336.
76. Zhang, H. M., Fischer, G., and Wydrzynski, T. (1998) Room-Temperature Vibrational Difference Spectrum for $S_2Q_B^-/S_1Q_B$ of Photosystem II Determined by Time-Resolved Fourier Transform Infrared Spectroscopy. *Biochemistry 37*, 5511−5517.
77. Chu, H.-A., Hillier, W., Law, N. A., Sackett, H., Haymond, S., and Babcock, G. T. (2000) Light-Induced FTIR Difference Spectroscopy of the S_2 to S_3 Transition of the Oxygen-Evolving Complex in Photosystem II. *Biochim. Biophys. Acta 1459*, 528−532.
78. Kimura, Y., Hasegawa, K., and Ono, T.-A. (2002) Characteristic Changes of the S_2/S_1 Difference FTIR Spectrum Induced by Ca^{2+} Depletion and Metal Cation Substitution in the Photosynthetic Oxygen-Evolving Complex. *Biochemistry 41*, 5844−5853.
79. Hasegawa, K., Kimura, Y., and Ono, T.-A. (2002) Chloride Cofactor in Photosynthetic Oxygen-Evolving Complex studied by FTIR Spectroscopy. *Biochemistry 41*, 13839−13850.
80. Kimura, Y., and Ono, T.-A. (2003) Functional and Structural Study on Chelator-Induced Supression of S_2/S_1 FTIR Spectrum in Photosynthetic Oxygen-Evolving Complex. *J. Inorg. Biochem. 97*, 231−239.
81. Christen, G., Seeliger, A. G., and Renger, G. (1999) P_{680}^+ Reduction Kinetics and Redox Transition Probability of the Water Oxidizing Complex as a Function of the pH and the H/D Isotope Exchange in Spinach Thylkoids. *Biochemistry 38*, 6082−6092.
82. Isgandarova, S., Renger, G., and Messinger, J. (2003) Functional Differences of Photosystem II from *Synechococcus elongatus* and Spinach Characterized by Flash Induced Oxygen Evolution Patterns. *Biochemistry 42*, 8929−8938.
83. Roelofs, T. A., Liang, W., Latimer, M. J., Cinco, R. M., Rompel, A., Andrews, J. C., Sauer, K., Yachandra, V. K., and Klein, M. P. (1996) Oxidation States of the Manganese Cluster During the Flash-Induced S-state Cycle of the Photosynthetic Oxygen-Evolving Complex. *Proc. Natl. Acad. Sci. U.S.A. 93*, 3335−3340.
84. De Wijn, R., Schrama, T., and van Gorkom, H. J. (2001) Secondary Stabilization Reactions and Proton-Coupled Electron Transport in Photosystem II Investigated by Electroluminescence and Fluorescence Spectroscopy. *Biochemistry 40*, 5821−5834.
85. De Wijn, R., and van Gorkom, H. J. (2002) S-state Dependence of the Miss Probability in Photosystem II. *Photosynth. Res. 72*, 217−222.
86. Steenhuis, J. J., and Barry, B. A. (1997) Protein and Ligand Environments of the S_2 state in Photosynthetic Oxygen Evolution: A Difference FT-IR study. *J. Phys. Chem. B 101*, 6652−6660.
87. Steenhuis, J. J., and Barry, B. A. (1998) Difference FT-IR studies of Photoassembly in the Manganese-Containing Catalytic Site of Photosystem. *J. Phys. Chem. B 102*, 4−8.
88. Steenhuis, J. J., Hutchison, R. S., and Barry, B. A. (1999) Alterations in Carboxylate Ligation at the Active Site of Photosystem II. *J. Biol. Chem. 274*, 14609−14616.
89. Hutchison, R. S., Steenhuis, J. J., Yocum, C. F., Razeghifard, M. R., and Barry, B. A. (1999) Deprotonation of the 33-kDa, Extrinsic, Manganese-Stabilizing Subunit Accompanies Photooxidation of Manganese in Photosystem II. *J. Biol. Chem. 274*, 31987−31995.
90. Halverson, K. M., and Barry, B. A. (2003) Evidence for Spontaneous Structural Changes in a Dark-Adapted State of Photosystem II. *Biophys. J. 85*, 2581−2588.
91. Barry, B. A. (2000) FT-IR spectroscopic studies of the S state transitions. *Photosynth. Res. 65*, 197−198.
92. Mehrotra, R. C., and Bohra, R. (1983) *Metal Carboxylates*, pp 48−60, Academic Press, London, UK.
93. Nara, M., Torii, H., and Tasumi, M. (1996) Correlation between the Vibrational Frequencies of the Carboxylate Group and Types of its Coordination to a Metal Ion: An ab Initio Molecular Orbital Study. *J. Phys. Chem. 100*, 19812−19817.
94. Krimm, S., and Bandekar, J. (1986) Vibrational Spectroscopy and Conformation of Peptides, Polypeptides, and Proteins. *Adv. Protein Chem. 38*, 181−364.
95. Tadesse, L., Nazarbaghi, R., and Walters, L. (1991) Isotopically Enhanced Infrared Spectroscopy: A Novel Method for Examining Secondary Structure at Specific Sites in Conformationally Heterogeneous Peptides, *J. Am. Chem. Soc. 113*, 7036−7037.
96. Haris, P. I., Robillard, G. T., van Dijk, A. A., and Chapman, D. (1992) Potential of ^{13}C and ^{15}N Labeling for Studying Protein−Protein Interactions Using Fourier Transform Infrared Spectroscopy. *Biochemistry 31*, 6279−6284.
97. Zhang, M., Fabian, H., Mantsch, H. H., and Vogel, H. J. (1994) Isotope-Edited Fourier Transform Infrared Spectroscopy Studies of Calmodulin's Interaction with Its Target Peptides. *Biochemistry 33*, 10883−10888.
98. Noguchi, T., and Inoue, Y. (1995) Molecular Interactions of the Redox-Active Accessory Chlorophyll on the Electron-Donor Side of Photosystem II as Studied by Fourier Transform Infrared Spectroscopy. *FEBS Lett. 370*, 241−244.
99. Noguchi, T., Mitsuka, T., and Inoue, Y. (1994) Fourier Transform Infrared Spectrum of the Radical Cation of β-Carotene Photoinduced in Photosystem II. *FEBS Lett. 356*, 179−182.
100. Berthomieu, C., Hienerwadel, R., Boussac, A., Breton, J., and Diner, B. A. (1998) Hydrogen-Bonding of Redox-Active Tyrosine Z of Photosystem II Probed by FTIR Difference Spectroscopy. *Biochemistry 37*, 10547−10554.
101. Berthomieu, C., Nabedryk, E., Mäntele, W., and Breton, J. (1990) Characterization by FTIR Spectroscopy of the Photoreduction of the Primary Quinone Acceptor Q_A in Photosystem II. *FEBS Lett. 269*, 363−367.
102. Hienerwadel, R., Boussac, A., Breton, J., and Berthomieu, C. (1996) Fourier Transform Infrared Difference Study of $Tyrosine_D$ Oxidation and Plastoquinone Q_A Reduction in Photosystem II. *Biochemistry 35*, 15447−15460.
103. Zhang, H. M., Razeghifard, M. R., Fischer, G., and Wydrzynski, T. (1997) A Time-Resolved FTIR Difference Study of the Plastoquinone Q_A and Redox-Active Tyrosine Y_Z Interactions in Photosystem II. *Biochemistry 36*, 11762−11768.
104. Dejonghe, D., Andrianambinintsoa, S., Berger, G., and Breton, J. (1998) Light-Induced FTIR Difference Spectroscopy of Q_A Photoreduction in Photosystem II Core Particles in *Photosynthe-*

sis: Mechanisms and Effects (Garab, G., Ed.) Vol. II, pp 1121−1124, Kluwer Academic Publishers, Dordrecht, The Netherlands.
105. Faller, P., Pascal, A., and Rutherford, A. W. (2001) β-carotene redox reactions in photosystem II: Electron-transfer pathway. *Biochemistry 40*, 6431−6440.
106. Tracewell, C. A., Cua, A., Stewart, D. H., Bocian, D. F., and Brudvig, G. W. (2001) Characterization of Carotenoid and Chlorophyll Photooxidation in Photosystem II. *Biochemistry 40*, 193−203.
107. Tracewell, C. A., and Brudvig, G. W. (2003) Two Redox-Active β-Carotene Molecules in Photosystem II. *Biochemistry 42*, 9127−9136.
108. Noguchi, T., and Inoue, Y. (1995) Identification of Fourier Transform Infrared Signals from the Non-Heme Iron in Photosystem II. *J. Biochem. 118*, 9−12.
109. Hienerwadel, R., and Berthomieu, C. (1995) Bicarbonate Binding to the Non-Heme Iron of Photosystem II Investigated by Fourier Transform Infrared Difference Spectroscopy and ^{13}C-Labeled Bicarbonate. *Biochemistry 34*, 16288−16297.
110. Berthomieu, C., and Hienerwadel, R. (2001) Iron coordination in Photosystem II: Interaction between Bicarbonate and the Q_B pocket Studied by Fourier Transform Infrared Spectroscopy. *Biochemistry 40*, 4044−4052.
111. Berthomieu, C., Boussac, A., Mäntele, W., Breton, J., and Nabedryk, E. (1992) Molecular Changes following Oxidoreduction of Cytochrome *b*559 Characterized by Fourier Transform Infrared Difference Spectroscopy and Electron Paramagnetic Resonance: Photooxidation in Photosystem II and Electrochemistry of Isolated Cytochrome *b*559 and Iron Protoporphyrin IX-Bisimidazole Model Compounds. *Biochemistry 31*, 11460−11471.
112. Hienerwadel, R., Boussac, A., Breton, J., Diner, B. A., and Berthomieu, C. (1997) Fourier Transform Infrared Difference Spectroscopy of Photosystem II Tyrosine D using Site-Directed Mutagenesis and Specific Isotope Labeling. *Biochemistry 36*, 14712−14723.
113. Kim, S. Y., and Barry, B. A. (1998) Vibrational Spectrum Associated with the Reduction of Tyrosyl Radical D$^\bullet$ in Photosystem II: A Comparative Biochemical and Kinetic Study. *Biochemistry 37*, 13882−13892.
114. Kim, S. Y., Ayala, I., Steenhuis, J. J., Gonzalez, E. T., Razeghifard, M. R., and Barry, B. A. (1998) Infrared Spectroscopic Identification of the C−O Stretching Vibration Associated with the Tyrosyl Z$^\bullet$ and D$^\bullet$ Radicals in Photosystem II. *Biochim. Biophys. Acta 1366*, 331−354.
115. O'Malley, P. J. (2002) Density Functional Calculations Modelling Tyrosine Oxidation in Oxygenic Photosynthetic Electron Transfer. *Biochim. Biophys. Acta 1553*, 212−217.
116. Diner, B. A., Tang, X.-S., Zheng, M., Dismukes, G. C., Force, D. A., Randall, D. W., and Britt, R. D. (1995) Environment and Function of the Redox Active Tyrosines of Photosystem II in *Photosynthesis: From Light to Biosphere* (Mathis, P., Ed.) Vol. II, pp 229−234, Kluwer Academic Publishers, Dordrecht.
117. Faller, P., Rutherford, A. W., and Debus, R. J. (2002) Tyrosine D oxidation at cryogenic temperature in photosystem II. *Biochemistry 41*, 12914−12920.
118. Faller, P., Goussias, C., Rutherford, A. W., and Un, S. (2003) Resolving Intermediates in Biological Proton-Coupled Electron Transfer: A Tyrosyl Radical Prior to Proton Movement. *Proc. Natl. Acad. Sci. U.S.A. 100*, 8732−8735.
119. Reinman, S., and Mathis, P. (1981) Influence of Temperature on Photosystem II Electron-Transfer Reactions. *Biochim. Biophys. Acta 635*, 249−258.
120. Shigemori, K., Mino, H., and Kawamori, A. (1997) pH and Temperature Dependence of Tyrosine Z$^\bullet$ Decay Kinetics in Tris-treated PSII Particles Studied by Time-Resolved EPR. *Plant Cell Physiol. 38*, 1007−1011.
121. Kühne, H., and Brudvig, G. W. (2002) Proton-Coupled Electron Transfer Involving Tyrosine Z in Photosystem II. *J. Phys. Chem. B 106*, 8189−8196.
122. Deacon, G. B., and Phillips, R. J. (1980) Relationships between the Carbon−Oxygen Stretching Frequencies of Carboxylato Complexes and the Type of Carboxylate Coordination. *Coord. Chem. Rev. 33*, 227−250.
123. Tackett, J. E. (1989) FT-IR Characterization of Metal Acetates in Aqueous Solution. *Appl. Spectrosc. 43*, 483−489.
124. Nakamoto, K. (1997) *Infrared and Raman Spectra of Inorganic and Coordination Compounds, Part B: Applications in Coordination, Organometallic, and Bioinorganic Chemistry*, 5th ed., pp 59−62, John Wiley & Sons, New York.
125. Venyaminov, S. Yu., and Kalnin, N. N. (1990) Quantitative IR Spectrophotometry of Peptide Compounds in Water (H_2O) Solutions. 1. Spectral Parameters of Amino Acid Residue Absorption Bands. *Biopolymers 30*, 1243−1257.
126. Barth, A. (2000) The Infrared Absorption of Amino Acid Side Chains. *Prog. Biophys. Mol. Biol. 74*, 141−173.
127. Rahmelow, K., Hübner, W., and Ackermann, Th. (1998) Infrared Absorbances of Protein Side Chains. *Anal. Biochem. 257*, 1−11.
128. Smith, J. C., Gonzalez-Vergara, E., and Vincent, J. B. (1997) Detection of Structural Changes upon Oxidation in Multinuclear Mn-Oxo-Carboxylate Assemblies by Fourier Transform Infrared Spectroscopy: Relationship to Photosystem II. *Inorg. Chim. Acta 255*, 99−103.
129. Czarnecki, K., Kirmaier, C., Holten, D., and Bocian, D. F. (1999) Vibrational and Photochemical Consequences of an Asp Residue Near the Photoactive Accessory Bacteriochlorophyll in the Photosynthetic Reaction Center. *J. Phys. Chem. A 103*, 2235−2246.
130. Tommos, C., Hoganson, C. W., Di Valentin, M., Lydakis-Simantiris, N., Dorlet, P., Westphal, K., Chu, H.-A., McCracken, J., and Babcock, G. T. (1998) Manganese and Tyrosyl Radical Function in Photosynthetic Oxygen Evolution. *Curr. Opin. Chem. Biol. 2*, 244−252.
131. Tommos, C. (2002) Electron, Proton, and Hydrogen-Atom Transfers in Photosynthetic Water Oxidation. *Philos. Trans. R. Soc. London, Ser. B 357*, 1383−1394.
132. Saygin, Ö., and Witt, H. T. (1984) On the Change of the Charges in the Four Photoinduced Oxidation Steps of the Water-Splitting Enzyme System S: Optical Characterization at O_2-Evolving Complexes Isolated from *Synechococcus*. *FEBS Lett. 176*, 83−87.
133. Saygin, Ö., and Witt, H. T. (1985) Evidence for the Electrochromic Identification of the Change of Charges in the Four Oxidation Steps of the Photoinduced Water Cleavage in Photosynthesis. *FEBS Lett. 187*, 224−226.
134. Rappaport, F., Blanchard-Desce, M., and Lavergne, J. (1994) Kinetics of Electron Transfer and Electrochromic Change During the Redox Transitions of the Photosynthetic Oxygen-Evolving Complex. *Biochim. Biophys. Acta 1184*, 178−192.
135. Kretschmann, H., Schlodder, E., and Witt, H. T. (1996) Net Charge Oscillation and Proton Release During Water Oxidation in Photosynthesis: An Electrochromic Band Shift Study at pH = 5.5−7.0. *Biochim. Biophys. Acta 1274*, 1−8.
136. Mulkidjanian, A., Cherepanov, D., Haumann, M., and Junge, W. (1996) Photosystem II of Green Plants: Topology of Core Pigments and Redox Cofactors as Inferred from Electrochromic Difference Spectra. *Biochemistry 35*, 3093−3107.
137. Ahlbrink, R., Haumann, M., Cherepanov, D., Bögershausen, O., Mulkidjanian, A., and Junge, W. (1998) Function of Tyrosine-Z in Water Oxidation by Photosystem II: Electrostatical Promotor instead of Hydrogen Abstractor. *Biochemistry 37*, 1131−1142.
138. Rappaport, F., and Lavergne, J. (1991) Proton Release During Successive Oxidation Steps of the Photosynthetic Water Oxidation Process: Stoichiometries and pH Dependence. *Biochemistry 30*, 10004−10012.
139. Schlodder, E., and Witt, H. T. (1999) Stoichiometry of Proton Release from the Catalytic Center in Photosynthetic Water Oxidation − Reexamination by a Glass Electrode Study at pH 5.5−7.2. *J. Biol. Chem. 274*, 30387−30392.
140. Rappaport, F., and Lavergne, J. (2001) Coupling of Electron and Proton Transfer in the Photosynthetic Water Oxidase. *Biochim. Biophys. Acta 1503*, 246−259.
141. Junge, W., Haumann, M., Ahlbrink, R., Mulkidjanian, A., and Clausen, J. (2002) Electrostatics and Proton Transfer in Photosynthetic Water Oxidation, *Philos. Trans. R. Soc. London, Ser. B 357*, 1407−1418.
142. Brettel, K., Schlodder, E., and Witt, H. T. (1984) Nanosecond Reduction Kinetics of Photooxidized Chlorophyll a_{II} (P-680) in Single Flashes as a Probe for the Electron Pathway, H^+-Release and Charge Accumulation in the O_2-Evolving Complex. *Biochim. Biophys. Acta 766*, 403−415.
143. Meyer, B., Schlodder, E., Dekker, J. P., and Witt, H. T. (1989) O_2 Evolution and Chl a_{II}^+ (P-680$^+$) Nanosecond Reduction Kinetics in Single Flashes as a Function of pH. *Biochim. Biophys. Acta 974*, 36−43.
144. Jeans, C., Schilstra, M. J., and Klug, D. R. (2002) The Temperature Dependence of P_{680}^+ Reduction in Oxygen-Evolving Photosystem. *Biochemistry 41*, 5015−5023.

145. Zhao, X. G., Richardson, W. H., Chen, J.-L., Li, J., Noodleman, L., Tsai, H.-L., and Hendrickson, D. N. (1997) Density Functional Calculations of Electronic Structure, Charge Distribution, and Spin Coupling in Manganese-Oxo Dimer Complexes. *Inorg. Chem. 36*, 1198−1217.
146. McGrady, J. E., and Stranger, R. (1997) Redox-Induced Changes in the Geometry and Electronic Structure of Di-μ-Oxo-Bridged Manganese Dimers. *J. Am. Chem. Soc. 119*, 8512−8522.
147. Delfs, C. D., and Stranger, R. (2001) Oxidation State Dependence of the Geometry, Electronic Structure, and Magnetic Coupling in Mixed Oxo- and Carboxylato-Bridged Manganese Dimers. *Inorg. Chem. 40*, 3061−3076.
148. Barone, V., Bencini, A., Gatteschi, D., and Totti, F. (2002) DFT Description of the Magnetic Properties and Electron Localization in Dinuclear Di-μ-Oxo-Bridged Manganese Complexes. *Chem. Eur. J. 8*, 5019−5027.

BI035915F